Chemical Engineering Science 229 (2021) 116133

Contents lists available at ScienceDirect

Chemical Engineering Science

journal homepage: www.elsevier.com/locate/ces

Review

Estimation of the dissipation rate of turbulent kinetic energy: A review

Guichao Wang [a,*], Fan Yang [a], Ke Wu [a], Yongfeng Ma [b], Cheng Peng [c], Tianshu Liu [d], Lian-Ping Wang [b,c,*]

[a] SUSTech Academy for Advanced Interdisciplinary Studies, Southern University of Science and Technology, Shenzhen 518055, PR China
[b] Guangdong Provincial Key Laboratory of Turbulence Research and Applications, Center for Complex Flows and Soft Matter Research and Department of Mechanics and Aerospace Engineering, Southern University of Science and Technology, Shenzhen 518055, Guangdong, China
[c] Department of Mechanical Engineering, 126 Spencer Laboratory, University of Delaware, Newark, DE 19716-3140, USA
[d] Department of Mechanical and Aeronautical Engineering, Western Michigan University, Kalamazoo, MI 49008, USA

HIGHLIGHTS

- Estimate of turbulent dissipation rate is reviewed.
- Experimental works are summarized in highlight of spatial/temporal resolution.
- Data processing methods are compared.
- Future directions in estimating turbulent dissipation rate are discussed.

ARTICLE INFO

Article history:
Received 8 July 2020
Received in revised form 27 August 2020
Accepted 8 September 2020
Available online 12 September 2020

Keywords:
Turbulent dissipation rate
Hot wire
LDV
PIV
PTV
Resolution

ABSTRACT

A comprehensive literature review on the estimation of the dissipation rate of turbulent kinetic energy is presented to assess the current state of knowledge available in this area. Experimental techniques (hot wires, LDV, PIV and PTV) reported on the measurements of turbulent dissipation rate have been critically analyzed with respect to the velocity processing methods. Traditional hot wires and LDV are both a point-based measurement technique with high temporal resolution and Taylor's frozen hypothesis is generally required to transfer temporal velocity fluctuations into spatial velocity fluctuations in turbulent flows. Multi probes of hot wires and multi points LDV could be used to measure velocity spatial gradients for a direct calculation of turbulent dissipation rate from its definition. Nevertheless, only PIV and PTV could provide simultaneous measurements of the distribution of turbulent dissipation rate in a turbulent field. These methods all suffer from the deficiency of spatial resolution as velocity measurements are required to resolve down to Kolmogorov scales for a strictly direct calculation of turbulent dissipation rate from fluctuating velocity gradients. To eliminate the necessity of resolving down to Kolmogorov scales, a large eddy simulation analogy and Smagorinsky model could be used for estimating the unresolved small scales, but Smagorinsky constant acts as an adjustment parameter at this stage. Different velocity processing methods are compared in the estimation of turbulent dissipation rate. The estimation of turbulent dissipation rate using structure function, energy spectrum and dimensional analysis methods could reduce the effects of low resolution, but it only provides temporal or spatial mean turbulent dissipation rate. Nevertheless, the field of turbulent dissipation rate, which is not distributed homogeneously, has intermittent spatio-temporal nature. The aim of this paper is to review the developments and limitations of the existing experimental techniques and different calculating methods and identify the future directions in successfully estimating turbulent dissipation rate in turbulent multiphase flows.

* Corresponding authors at: Guangdong Provincial Key Laboratory of Turbulence Research and Applications, Center for Complex Flows and Soft Matter Research and Department of Mechanics and Aerospace Engineering, Southern University of Science and Technology, Shenzhen 518055, Guangdong, China (L.-P. Wang).
E-mail addresses: guichao.wang@uon.edu.au (G. Wang), wanglp@sustech.edu.cn (

https://doi.org/10.1016/j.ces.2020.116133
0009-2509/

Contents

1. Introduction

The applications of turbulence in the engineering field have long been studied for its critical role in momentum transport (Davies, 2012), dispersion and mixing (Gollub et al., 1991), heat and mass transport (Kader and Yaglom, 1972), and surface drag (Choi et al., 1994). Especially in chemical engineering, turbulent flows determine the heat and mass transfer, affecting chemical reaction and performance of chemical processes (Deshpande et al., 2009). Micromixing has been recognized as the limiting time scale in these processes (Bałdyga and Pohorecki, 1995). Micromixing occurs at small scales, which can be predicted from the turbulent kinetic energy and its dissipation rate. The dissipation rate of turbulent kinetic energy, which will be referred to as turbulent dissipation rate in the following, is a key parameter to quantify the level of turbulence, the resulted mixing and the turbulent transport properties.

It was considered that the small eddies controlled the transport phenomena at the interface for the reason that smaller eddies contributed more to the interfacial turbulence and promoted mixing at the interface. (Banerjee et al., 1968; Lamont and Scott, 1970). The mass transfer behavior was linked to the hydrodynamic behavior near the surface in a way that surface renewal was controlled by turbulent eddies. Eddies of various sizes were related to the turbulent energy spectrum by using the energy dissipation rate following the Kolmogorov's hypothesis (Kolmogorov, 1941a). Therefore, the effects of turbulence on heat and mass transfer are accounted by incorporating the turbulent dissipation rate that was estimated from the bulk turbulence energy spectrum.

The hydrodynamics of multiphase flows is dependent on the level of turbulent dissipation rate, which is represented in coalescence and break-up of bubbles or droplets (Davies, 1985; Luo and Svendsen, 1996; Prince and Blanch, 1990; Sajjadi et al., 2013; Zhang et al., 2019; Zhou and Kresta, 1998), detachment of a bubble/particle (Wang et al., 2016a, 2016b, 2014a, 2014b), aggregation of particles (Wang et al., 2019), collisions of particles (Chen et al., 2019; Nguyen et al., 2016; Wan et al., 2020; Williams and Crane, 1983). The global values averaged in volume of turbulent dissipation rate can be easily calculated from the energy input into the system (Aloi and Cherry, 1996). This has been widely used in the conventional design of chemical process equipment. Turbulence in most chemical processes is anisotropic and inhomogeneous, which means that global energy dissipation is not equivalent to local energy dissipation (Kuzzay et al., 2015). Moreover, hydrodynamics in a piece of chemical equipment is generally inhomogeneous with turbulent dissipation rate varying considerably throughout the tank, and taking a stirred tank as an example, power is primarily dissipated in the region of the impeller (Kresta and Wood, 1991). It is the local turbulent dissipation rate that controls cell damage, drop breakup, heat transfer, mass transfer, etc. Therefore, characterizing the small-scale turbulent flow structures and the spatial distribution of turbulent dissipation rate in a chemical process is of prime importance to improve performance while designing new equipment based on the understanding of flow patterns.

Although significant studies are reported on the estimation of turbulent dissipation rate in chemical engineering processes, to the best of authors' knowledge there is no comprehensive review combining experimental techniques and data processing methods reported on this area to this date. It is worth noting that for last few decades estimating turbulent dissipation rate has also attracted attentions from researchers in the fields of marine environment and atmospheres (Cohn, 1995; Schacher et al., 1981; Wiles et al., 2006). Radar techniques have been applied to measure turbulent dissipation rates in lower stratosphere and middle atmosphere (Crane, 1980; Hermawan and Tsuda, 1999; Hocking, 1985). More recent work has been devoted to combining radiosonde observations with radar (Kohma et al., 2019), micropulse coherent lidar (Banakh et al., 2017), and acoustic Doppler current profiler (Ross and Lueck, 2005; Wiles et al., 2006). To avoid complexities of estimating turbulent dissipation rate in marines and atmospheres, this review is primarily restrained to the discussion of estimating turbulent kinetic energy dissipation in chemical processes where extreme discrepancy in spatial scales and different measurement techniques was found compared to researches in marines and atmospheres. This literature review tries to summarize previous studies on estimating turbulent dissipation rate with emphasis on in-depth analysis of the strength and weakness of different calculation methods, and on the comparison of the various experimental techniques reported. We did not intend to include

all such studies as a large number of studies on hydrodynamics in chemical processes would discuss a bit of turbulent dissipation rate. This paper aims to include representative examples in the estimation of turbulent dissipation rate.

2. Origin of turbulent dissipation rate

The equation of turbulence kinetic energy for constant viscosity and density can be written as

$$\frac{\bar{D}k}{\bar{D}t} = \frac{\partial}{\partial x_j}\left[-\frac{\langle u_j p'\rangle}{\rho} + 2\upsilon\langle u_i s_{ij}\rangle - \frac{1}{2}\langle u_i u_j u_j\rangle\right] - 2\upsilon\langle s_{ij}s_{ij}\rangle - \langle u_i u_j\rangle\langle S_{ij}\rangle \tag{1}$$

where the first term in the right-hand side (RHS) of the equation is the transport of turbulence kinetic energy by pressure, viscous stresses and Reynolds stresses, respectively. The second term is the rate of dissipation of turbulence kinetic energy and the last term is turbulence production. The dissipation rate of turbulent kinetic energy is defined from the Reynolds-averaged turbulent kinetic energy equation. Following the definition by Hinze (1975), the turbulent dissipation rate can be derived from the turbulent velocity gradients as:

$$\varepsilon = \frac{1}{2}\nu\overline{\left(\frac{\partial u_i}{\partial x_j} + \frac{\partial u_j}{\partial x_i}\right)^2} \tag{2}$$

where ν is the kinematic viscosity, u is the fluctuating velocity, and the subscripts i, j, k represent the three Cartesian directions. This equation can be developed in three directions and can be written as:

$$\varepsilon = \nu\left\{\begin{array}{c} 2\overline{\left(\frac{\partial u}{\partial x}\right)^2} + \overline{\left(\frac{\partial v}{\partial x}\right)^2} + \overline{\left(\frac{\partial w}{\partial x}\right)^2} + \overline{\left(\frac{\partial u}{\partial y}\right)^2} \\ +2\overline{\left(\frac{\partial v}{\partial y}\right)^2} + \overline{\left(\frac{\partial w}{\partial y}\right)^2} + \overline{\left(\frac{\partial u}{\partial z}\right)^2} + \overline{\left(\frac{\partial v}{\partial z}\right)^2} \\ +2\overline{\left(\frac{\partial w}{\partial z}\right)^2} + 2\left(\overline{\left(\frac{\partial u}{\partial y}\right)\left(\frac{\partial v}{\partial x}\right)} + \overline{\left(\frac{\partial u}{\partial z}\right)\left(\frac{\partial w}{\partial x}\right)} + \overline{\left(\frac{\partial v}{\partial z}\right)\left(\frac{\partial w}{\partial y}\right)}\right) \end{array}\right\} \tag{3}$$

It has nine squared fluctuating velocity gradients and three cross-product velocity gradients. From the definition, turbulent dissipation rate is determined from kinetic viscosity and fluctuating velocity gradients.

When Reynolds number is sufficiently high, the turbulent dissipation rate in the energy cascade is a constant of order unity when scaled on the integral scale and root-mean-square velocity (Sreenivasan, 1998; Sreenivasan and Antonia, 1997). The scaling of the turbulence energy dissipation rate regards that the time scale of the energy dissipation rate in fully turbulent flows is of the same order of magnitude as the characteristic time scale of the energy containing eddies (Sreenivasan, 1984). Turbulent dissipation rate remains constant with increasing Reynolds number when turbulence is intensified and the viscous forces are reduced relative to the inertial forces (Taylor, 1935). Upper bounds on the turbulent dissipation rate were given for shear driven turbulence and body-forced turbulence (Doering and Constantin, 1992; Doering and Foias, 2002).

The turbulent kinetic energy cascades from large scales to small scales, which will be dissipated into heat when the scales are sufficiently small for viscous dissipation to be effective (Richardson, 2007). The dissipative length scale is determined from mean rate of dissipation of the turbulent kinetic energy, ε, and the kinematic viscosity, ν, in the form as $(\nu^3/\varepsilon)^{1/4}$. Dissipation should be considered a random quantity with its own probability distribution, which reveals strong fluctuations in the time and space domains (Elsner and Elsner, 1996). In highly turbulent flows, intermittency is seen in the irregular dissipation of kinetic energy (Meneveau and Sreenivasan, 1991). Intermittency of the turbulent dissipation rate ε was investigated experimentally that the dissipation field had a multifractal distribution (Boffetta and Romano, 2002; Meneveau and Sreenivasan, 1991). Tsinober et al. (1992) considered that the instantaneous dissipation rate had a log-normal distribution. Though there has not been a consensus on the distribution of dissipation, it is well accepted that the highly intermittent spatio-temporal nature of the field of turbulent dissipation rate can be described in terms of a corresponding instantaneous fluctuating dissipation scale (Morshed et al., 2013). Regions of intense rotation and energy dissipation were shown to be greatly correlated, with intermittent events clustered in the periphery of larger scale vortices (Worth and Nickels, 2011). The regions of intense dissipation tended to present a sheet-like shape, which was closely linked with the occurrence of the vortical structures (Ganapathisubramani et al., 2007, 2008). Flow structures were connected to the production and dissipation of turbulent kinetic energy. Zaripov et al. (2020) found strong dissipation was caused by strong rotation motion of vortical structures near the wall in the study of the extreme manifestation of turbulent dissipation rate in turbulent channel flow. Therefore, the Kolmogorov length scale representing dissipation scales does not reflect the intermittent nature of ε as it is calculated from the mean dissipation rate (Bailey and Witte, 2016).

It was shown that singularities may induce additional energy dissipation by inertial means (Saw et al., 2016). The inertial energy dissipation was estimated and local events of extreme values were identified in a turbulent swirling flow using a stereoscopic particle image velocimetry. The topology of extreme events of inertial dissipation was associated with special configurations of eigenvalues of the velocity strain tensors around critical points of flow patterns where the velocity fronts, saddle points, spirals, jets and, in some cases, suggestive of cusps were located. This indicates the non-trivial structures of sub-Kolmogorov flows which could be possible footprints of singularities of the Navier–Stokes equation. Sub-Kolmogorov-scale fluctuations in fluid turbulence was related to a whole range of local dissipation scales (Schumacher, 2007). It is confirmed by Zeff et al. (2003) that intense dissipation events were generally a typical sequence begins with rapid strain growth, followed by rising vorticity and a final sudden decline in stretching. Therefore, it is fundamental to measure the velocity gradient tensor in turbulent flows for the estimation of turbulent dissipation rate (Wallace and Vukoslavčević, 2010).

3. Velocity processing methods for turbulent dissipation rate

3.1. Fluctuating velocity gradients

Turbulent dissipation rate could be directly calculated from its definition expressed in Eq. (3). To directly determine the turbulent dissipation rate, the gradients in three directions of three fluctuating velocities should be measured. While it is routinely done in direct numerical simulations (DNS) of turbulence (Wang et al., 1996), this is a difficult task for all velocity measurement techniques. This difficulty appears as apparent inconsistencies of measured small-scale statistics such as that between the measured enstrophy production and velocity gradient skewness. With limited number of velocity gradients that can be measured, several simplifications have to be made to calculate turbulent dissipation rates from fluctuating velocity gradients. For the simplest turbulence, i.e. homogeneous and isotropic turbulence, the dissipation rate can be calculated from one velocity gradients as:

$$\varepsilon_i = 15\nu\overline{\left(\frac{\partial u_i}{\partial x_i}\right)^2} \tag{4}$$

Under Taylor's hypothesis for frozen turbulence pattern (Taylor, 1938), turbulent dissipation rate could be calculated from time series of fluctuating velocity. It is written as:

$$\varepsilon_i = \frac{15\nu}{U_1^2}\overline{\left(\frac{\partial u}{\partial t}\right)^2} \tag{5}$$

where U_1 is the mean streamwise velocity component. It only holds when fluctuating velocity is small compared to the mean velocity. Sharp et al. (2001, 2000) considered turbulence as statistically isotropic, but non-homogeneous. The unknown velocity gradients were estimated from the measured ones, and the dissipation rate defined by Eq. (3) can be simplified as:

$$\varepsilon = \nu\left(2\overline{\left(\frac{\partial u}{\partial x}\right)^2} + 2\overline{\left(\frac{\partial v}{\partial y}\right)^2} + 3\overline{\left(\frac{\partial v}{\partial x}\right)^2} + 3\overline{\left(\frac{\partial u}{\partial y}\right)^2} + 2\overline{\frac{\partial u}{\partial y}\frac{\partial v}{\partial x}}\right) \tag{6}$$

Turbulent dissipation rates estimated from Eq. (6) are better than that calculated from Eq. (4). For some situations, the assumption of isotropic turbulence does not apply. When the small-scale turbulence can be assumed as locally axisymmetric, according to Antonia et al. (2006) and George and Hussein (2006), turbulent dissipation rate can be expressed as:

$$\varepsilon = \nu\left(\overline{\left(\frac{\partial u}{\partial x}\right)^2} + \overline{8\left(\frac{\partial v}{\partial y}\right)^2} + \overline{2\left(\frac{\partial v}{\partial x}\right)^2} + \overline{2\left(\frac{\partial u}{\partial y}\right)^2}\right) \tag{7}$$

It should be pointed out that the directly estimated turbulent dissipation rate from fluctuating velocity gradients with the assumptions of isotropy, local isotropy or local axisymmetry decreased as interrogation size increased (Xu and Chen, 2013). To a large extent, this is affected by the resolution of measurements.

3.2. Smagorinsky closure method

When a dynamic equilibrium between the energy transferred from largest scales to smallest scales is achieved, the turbulent dissipation rate could be estimated from the flux of turbulent kinetic energy through the inertial subrange (Ducci and Yianneskis, 2005). This is the cornerstone of using Smagorinsky sub-grid model in large eddy particle image velocimetry (PIV) for the estimation of turbulent dissipation rate. The apparent advantage of this method is that velocity measurements does not need to resolve the Kolmogorov scales. The turbulent dissipation rate could be approximated as subgrid scale dissipation rate at the PIV resolution, which can be written as:

$$\varepsilon = \frac{1}{2}\overline{\nu_T\left(\frac{\partial u_i}{\partial x_j} + \frac{\partial u_j}{\partial x_i}\right)^2} \tag{8}$$

where ν_T is turbulent viscosity. It can be computed from the measured turbulent velocity gradients. It is

$$\nu_T = (C_s\Delta)^2\left[\frac{1}{2}\left(\frac{\partial u_i}{\partial x_j} + \frac{\partial u_j}{\partial x_i}\right)^2\right]^{1/2} \tag{9}$$

where Δ is the grid scale corresponding to the PIV spatial resolution, C_s is the Smagorinsky constant. Turbulent dissipation rate is:

$$\varepsilon = (C_s\Delta)^2\left\{\begin{array}{c} 2\overline{\left(\frac{\partial u}{\partial x}\right)^2} + \overline{\left(\frac{\partial v}{\partial x}\right)^2} + \overline{\left(\frac{\partial w}{\partial x}\right)^2} + \overline{\left(\frac{\partial u}{\partial y}\right)^2} \\ +2\overline{\left(\frac{\partial v}{\partial y}\right)^2} + \overline{\left(\frac{\partial w}{\partial y}\right)^2} + \overline{\left(\frac{\partial u}{\partial z}\right)^2} + \overline{\left(\frac{\partial v}{\partial z}\right)^2} \\ +2\overline{\left(\frac{\partial w}{\partial z}\right)^2} + 2\left(\overline{\left(\frac{\partial u}{\partial y}\right)\left(\frac{\partial v}{\partial x}\right)} + \overline{\left(\frac{\partial u}{\partial z}\right)\left(\frac{\partial w}{\partial x}\right)} + \overline{\left(\frac{\partial v}{\partial z}\right)\left(\frac{\partial w}{\partial y}\right)}\right) \end{array}\right\}^{3/2} \tag{10}$$

Note that it has not reached a consensus on the value of Smagorinsky constant. Sheng et al. (2000) used a value of 0.17; Sharp and Adrian (2001) selected a value of 0.21; Gabriele et al. (2009) suggested a value of 0.11. It is suggested that the value should be chosen according to the ratio between the spatial resolution and the Kolmogorov scale (Meyers and Sagaut, 2006). Bertens et al. (2015) considered that the Smagorinsky constant for PIV measurements should be dependent on the measurement conditions, likewise the interrogation widow overlap, the used elements of the strain tensor and the way in which derivatives are approximated. Most of the work is done with 2-D PIV and only five out of twelve terms in the definition of turbulent dissipation rate could be determined. The assumptions of isotropic or axisymmetric flow should be made to estimate the turbulent dissipation rate using large eddy PIV.

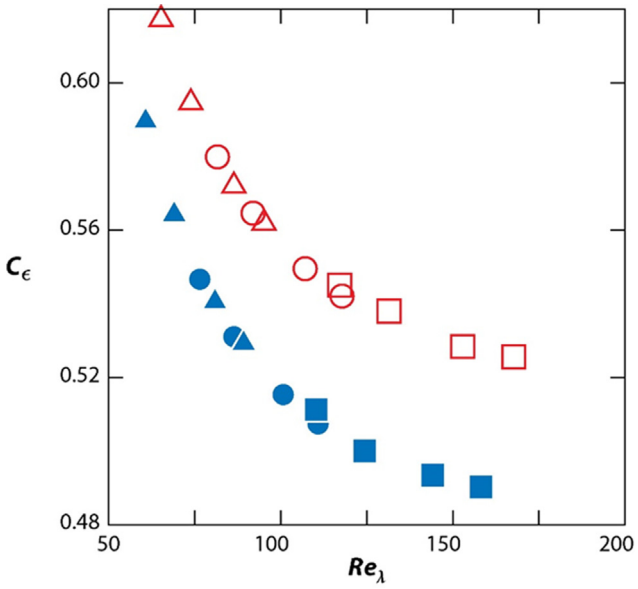

Fig. 1. C_ε as a function of Re_λ from DNS of forced periodic stationary turbulence with closed and open symbols corresponding to different large-scale forcing procedures (Goto and Vassilicos, 2009; Vassilicos, 2015).

3.3. Dimensional analysis

Batchelor (1953) suggested the form of turbulent dissipation rate based on dimensional analysis. The mechanism of turbulence dissipation originates from the Richardson-Kolmogorov cascade under the assumption that turbulence is at equilibrium. From the equilibrium cascade, the rate at which kinetic energy crosses a length scale is the same from the largest scale to the smallest length scale (Mouri et al., 2012; Vassilicos, 2015). The rate of transfer of energy can be characterized by fluctuating velocity, u' over integral length scale, l_e. The energy, that is transferred, is turbulence kinetic energy u'^2. Therefore, the turbulent dissipation rate can be written as:

$$\varepsilon = \frac{C_\varepsilon u'^3}{l_e} \tag{11}$$

where C_ε is a constant originating from the consequence of equilibrium assumption (Kolmogorov, 1941a, 1941c). Though the dimensionless dissipation rate was experimentally found nearly a constant for sufficiently high values of Taylor Reynolds number (Puga and LaRue, 2017), this assumption should not be taken lightly (Tennekes et al., 1972). It is found that C_ε is not universal, which is dependent on the initial conditions, inlet/boundary conditions and the type of flow (Antonia and Pearson, 2000; Bos and Rubinstein, 2017; Bos et al., 2007). Even in statistically stationary isotropic turbulence, time lag between energy injection and energy dissipation should be considered when C_ε is estimated at a specific time step

(Pearson et al., 2004). Valente and Vassilicos (2012) experimentally showed that the C_ε followed $f(Re_M)/Re_L$ during the decay of grid-generated turbulence, with Re_M as global Reynolds number and Re_L as local Reynolds number. This has been confirmed by results from other independent grid-turbulence experiments (Hearst and Lavoie, 2014; Isaza et al., 2014; Seoud and Vassilicos, 2007) and DNS simulations (Nagata et al., 2013; Sreenivasan, 1998) that C_ε is a function of Reynolds number as is shown in Fig. 1. McComb et al. (2015) explained that the decay of dimensionless dissipation with increasing Reynolds number was because of the increase in the Taylor surrogate.

Integral length scale represents the correlation distance of velocity components in space and can be calculated from the integration of velocity correlation function which requires the simultaneous measurements of the velocities at two different positions. When Taylor's frozen hypothesis is applied, the velocity at a different position could be estimated from the time series of velocity measurements at one point (Taylor, 1938). Costes and Couderc (1988) assumed that the integral length scaled as the diameter of tank and Calabrese and Stoots (1989) assumed the integral length to scale as the half diameter of tank. Kresta and Wood (1993) regarded that the dimensional analysis method gave accurate results for l_e assumed as one tenth of the diameter of a stirred tank and the constant C_ε assumed equal to one. Wu et al. (1989) approximated above equation to estimate the distribution of turbulent dissipation rates in a stirred tank using LDV as:

$$\varepsilon = \frac{C_\varepsilon u_r'^3}{\tau\sqrt{\bar{U}_r^{-2} + u_r'^2}} \tag{12}$$

where $\tau = L_r/\bar{U}_c; \bar{U}_c = \sqrt{\bar{U}^2 + u'^2}; C_\varepsilon = 1$. The subscript r represents radial direction. According to Wu et al. (1989), the underlined assumptions using above equation to estimate local turbulent dissipation rates are: (1) energy cascade from large vortices to small vortices; (2) local equilibrium between turbulence production and dissipation; (3) local isotropy of small scales. Wu and Patterson (1989) further quantified constant A as 0.85. Zhou and Kresta (1996a) simplified l_e as one tenth of the diameter of a stirred tank. Schäfer et al. (1997) calculated the integral length scale from an energy balance calculation throughout the tank and a value of 1/8.71 tank diameter was achieved. Gabriele et al. (2009) used 2-D spatial autocorrelation to calculate integral length scale for the estimate of local turbulent dissipation rate from dimensional analysis using local fluctuating velocity. There is a wide variation in the assumed integral length scale and, moreover, there is no consensus on the choice of constant C_ε. More analysis is needed on the choice of these values for specific applications.

3.4. Structure function

In the inertial subrange, the turbulent dissipation rate is connected to the velocity structure functions under the Kolmogorov second similarity hypothesis (Kolmogorov, 1941b). The second order velocity structure function is defined as:

$$D_{ij}(r,t) = \left\langle \left(u_i(x+r,t) - u_i(x,t)\right)\left(u_j(x+r,t) - u_j(x,t)\right)\right\rangle \tag{13}$$

The second-order velocity structure function in the longitudinal direction is:

$$D_{LL}(r,t) = \left\langle \left(u_1(x+r,t) - u_1(x,t)\right)^2\right\rangle \tag{14}$$

The second-order longitudinal velocity structure function is a function of turbulent dissipation rate in the inertial subrange, in the form as:

$$D_{LL}(r,t) = C_2(\varepsilon r)^{2/3} \tag{15}$$

where C_2 is a universal constant according to Sreenivasan (1995) and a value of 2.12 was determined. The third-order longitudinal velocity structure function is a function of turbulent dissipation rate in the inertial subrange, in the form as:

$$D_{LLL}(r,t) = C_3\varepsilon r \tag{16}$$

Kolmogorov (1941a) gave C_3 as −0.8. De Jong et al. (2009) assumed that coefficients C_2 and C_3 were dependent on the Reynolds number based on the Taylor microscale. This has been considered as major contributors to the underestimation of turbulent dissipation rate.

3.5. Energy spectrum

The Kolmogorov second similarity hypothesis (Kolmogorov, 1941b) considers the longitudinal energy spectrum in the inertial subrange in the following form:

$$E_{11}(k_1) = C_1\varepsilon^{2/3}k_1^{-5/3} \tag{17}$$

where C_1 is a universal empirical constant and the value is suggested to be 0.53 by Sreenivasan (1995). Turbulent dissipation rate can be determined from fitting the curve of energy spectra in a way that apply a $k_1^{-5/3}$ curve fit to the inertial subrange of E_{11}. It can be written as:

$$\varepsilon = \left(\frac{1}{C_1}k_1^{5/3}E_{11}(k_1)\right)^{3/2} \tag{18}$$

According to Pope (2001), $E_{11}(k_1)$ can be determined from the cosine transform of the longitudinal spatial correlation function. It can be written as:

$$E_{11}(k_1) = \frac{2}{\pi}\langle u_1'^2\rangle\int_0^\infty f(r_1)cos(k_1r_1)dr_1 \tag{19}$$

The longitudinal energy spectrum can also be obtained by performing a Fourier transform of PIV velocity data. According to Liu et al. (1994), $E_{11}(k_1)$ can be written as:

$$E_{11}\left(k_1\right) = \frac{1}{\triangle k_1}\frac{1}{N^2}\sum_{j=0}^{N/2-1}\widehat{u}_j\widehat{u}_j^* \tag{20}$$

where N is the number of points that are transformed, $\widehat{u}_j$ is the Fourier transform of u_1', and $\widehat{u}_j^*$ are the complex conjugate of the Fourier transform. The Fourier transform of PIV measurements are generally carried out using fast Fourier transform, which requires data to be periodic. The PIV measurements could be transformed periodically by forcing velocity to 0 at the limits of the view area (Hwang and Eaton, 2004).

3.6. Forced balance of the TKE equation

Azad and Kassab (1989) suggested that the local turbulent dissipation rate can be determined by solving turbulent kinetic energy equation as is showed in Eq. (1). By following turbulent kinetic energy balance, turbulent dissipation rate can be written in the following form

$$\varepsilon = \frac{\partial}{\partial x_j}\left[-\frac{\langle u_j p'\rangle}{\rho} + 2\upsilon\langle u_i s_{ij}\rangle - \frac{1}{2}\langle u_i u_j u_j\rangle\right] - \langle u_i u_j\rangle\langle S_{ij}\rangle - \frac{\partial}{\partial t}\left(\frac{1}{2}\bar{u_i'}\bar{u_i'}\right) - \bar{u_j}\frac{\partial}{\partial x_j}\left(\frac{1}{2}\bar{u_i'}\bar{u_i'}\right) \tag{21}$$

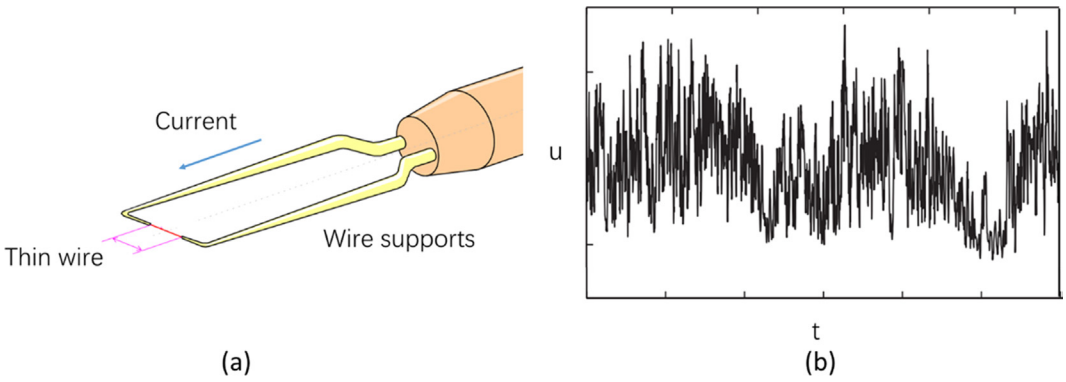

Fig. 2. (a) Schematic of standard hot-wire probe (b) Time series of velocity measured using a hot wire.

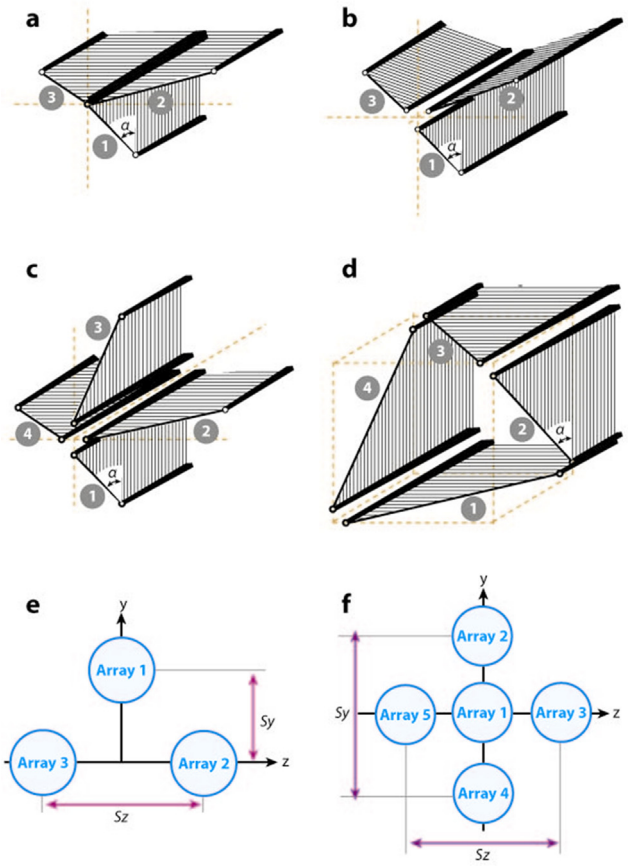

Fig. 3. Typical array and probe configurations: (a) T array, (b) orthogonal array, (c) plus array, (d) square array, (e) three-array probe, and (f) five-array probe (Wallace and Vukoslavčević, 2010).

Some assumptions have to be made to determine each terms, in particular the first term on the RHS of the equation representing pressure diffusion cannot be measured. The advantage of this method is that measurements of flow don't have to resolve down to the dissipative Kolmogorov scales. However, the disadvantage accompanied is that the estimated value of turbulent dissipation rate is affected by errors involved in the estimation of each terms. Escudié and Liné (2003) estimated the turbulent dissipation rate in a stirred tank from the balance equation of turbulent kinetic energy. Each term was derived from PIV measurements except the pressure diffusion term which cannot be calculated from the PIV data and was assumed to be negligible. The same method was also used to determine the fraction of total energy dissipated in the impeller region (Khan et al., 2006).

4. Experimental methods of measuring velocity for estimating ε

4.1. Hot wires

Measuring the turbulent dissipation rate using a hot-wire probe has been widely investigated and reported. The working principle is based on measuring the heat loss of the wire which is heated by electrical current. Critical reviews on the measurements of turbulent dissipation rate using hot wires has been presented (Antonia, 2003; Elsner and Elsner, 1996; Lekakis, 1996; Wallace and Vukoslavčević, 2010; Zhu and Antonia, 1996b). A brief summary is given here. The expression of turbulent dissipation rate in Eq. (3) could be simplified, following the local isotropy hypothesis (Kolmogorov, 1941b, 1962), to Eq. (4). Following Taylor's frozen flow hypothesis, velocities of temporal fluctuations could be transformed into spatial fluctuations in turbulent flows. Time series of velocity measured using hot wires could be used to estimate turbulent dissipation rate following Eq. (5). A single standard hot-wire probe is capable of measuring time series of velocity. Fig. 2(a) shows the schematic view of a standard hot-wire probe and Fig. 2 (b) shows the time series of velocity measured using a hot wire. The turbulent dissipation could also be estimated from energy spectrum obtained from time series of velocities measured using hot wires. The spectra corresponding to inertial ranges were used to obtain turbulent dissipation rate by the fitting of a $-5/3$ power law to the spectra (Lawn, 1971).

Direct measurement of streamwise derivative could be achieved by placing two hot wires on the same streamline. As is shown in Fig. 3, the geometry of a probe can be very complicated, which can be comprised of a number of arrays with each array consisted of sensors of different numbers and orientations (Wallace and Vukoslavčević, 2010). Browne et al. (1987) measured the nine major terms that make up the total dissipation using hot wires and X-wires in the self-preserving region of a cylinder wake. It was found that local isotropy was not satisfied and the isotropic dissipation was smaller than the total dissipation by about 45% on the wake centreline and by about 80% near the wake edge. Tsinober et al. (1992) developed a twelve-wire hot-wire probe to measure three velocity components and their nine gradients. Nevertheless, this arrangement will distort output signal from the second wire affected by the existence of the first wire as it is in the wake of the first (Elsner and Elsner, 1996). Generally, the multi-hot-wire technique, with more hot wires and complex geometry, has a deficiency of lower spatial resolution. The arrangements of hot wires were discussed in the estimation of mean and instantaneous turbulent dissipation rates (Antonia, 2003). The effects of wire length, separations between wires and effective wire inclinations were studied (Zhu and Antonia, 1996a, b), and expressions for correcting spectra and variances of velocity derivatives were presented.

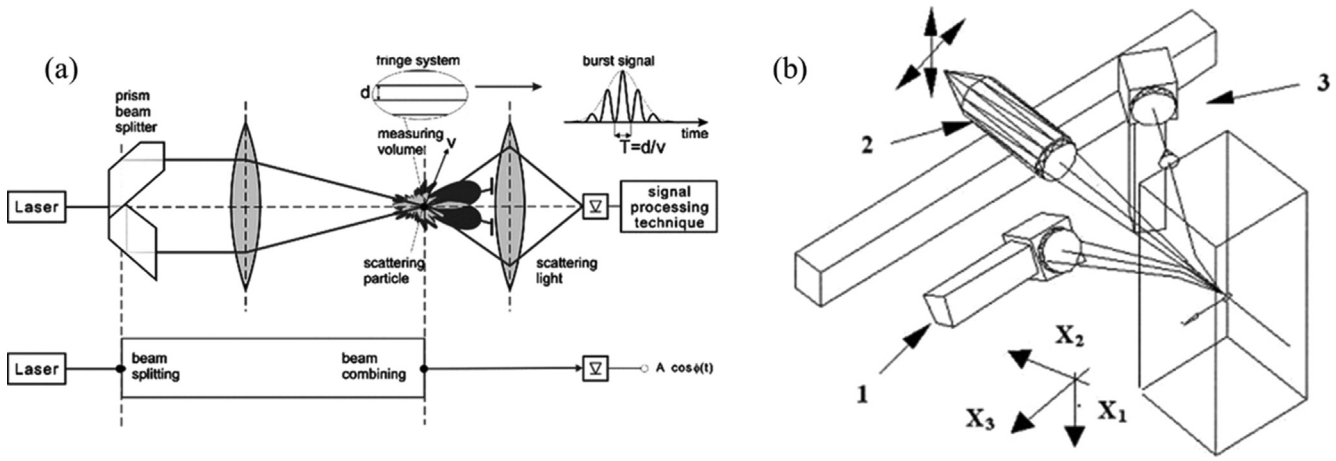

Fig. 4. (a) Schematic illustration of one point LDV (Czarske, 2006) (b) Probe arrangement of two-point LDV to measure the velocity gradients $(\partial u_1/\partial x_1)^2$, $(\partial u_1/\partial x_3)^2$, $(\partial u_3/\partial x_3)^2$, $(\partial u_3/\partial x_1)^2$ (Ducci and Yianneskis, 2005).

Special attention should be paid to the effect of the finite spatial resolution of hot-wire anemometry on the measurements of turbulence energy dissipation, especially when the smallest eddy is smaller than the wire length (Elsner et al., 1993). The zero wire length extrapolation technique allows one to bypass the spatial filtering effect of the finite length of the hot wire (Azad and Kassab, 1989). The turbulent dissipations could be calculated by extrapolating the values of dissipation obtained from different lengths of hot wires through the measurement of spectra to zero length. However, the idea of extrapolation to zero length of the hot wire assumes that the dissipation occurs at fine scale structures and these structures obey local isotropy. Puga and LaRue (2017) achieved time-resolved velocity measurements using a hot-wire in a nearly homogeneous and isotropic flow downstream of an active grid. It is found that the dimensionless dissipation rate was nearly a constant for sufficiently high values of Taylor Reynolds number, and is approximately equal to 0.87. Nevertheless, Pearson et al. (2002) did not find a universal value for the coefficient C_ε from data acquired using the hot-wire technique with a single-wire probe made of 1.27 mm diameter Wollaston wire. A universal value for this coefficient seem to be untenable as initial conditions and flow type have persistent influence on the normalized turbulent dissipation rate (Burattini et al., 2005).

4.2. Laser Doppler velocimetry

Laser Doppler Velocimetry (LDV), also named as Laser Doppler Anemometry, measures single point velocities in a transparent or semi-transparent fluid utilising the principle of Doppler Shift of laser beams which are reflected by seeding particles in the fluid media (Tropea, 1995). Fig. 4(a) shows schematic illustration of one point LDV. It would be straightforward to estimate turbulent dissipation rate using Eq. (1) from time series of velocity measured by LDV. Wu et al. (1989) pointed out that LDV was not suitable for using Eq. (5) as the size of the measuring volume was large compared to the small scale eddies responsible for the energy dissipation. This relatively large size caused the so-called ambiguity noise with a frequency range wider than the turbulence power spectrum, which resulted in turbulent dissipation rates approximately three orders of magnitude higher. 1-D LDV was used to measure the maximum turbulent dissipation rate for the study of the effect of tank geometry on the maximum dissipation (Zhou and Kresta, 1996b). It was found that 28.2% of the total energy was dissipated in the impeller discharge region, though it was only 4.87% of the total volume.

Kresta and Wood (1993) regarded that the dimensional analysis method gave accurate results for l_e assumed as one tenth of the diameter of a stirred tank and the constant C_ε assumed equal to one. They compared four methods in the estimation of turbulent dissipation rate using velocity information measured using LDV. The four methods were (1) the gradient hypothesis method using the constitutive equation from the k-ε model, (2) Taylor's hypothesis used to convert time derivatives to spatial derivatives, (3) dimensional arguments for the estimation of ε from k using a constant length scale, and (4) the autocorrelation coefficient function used to calculate the Eulerian integral time scale and then combine with k to estimate ε. Schäfer et al. (1997) followed the dimensional analysis method for the estimation of the distribution of turbulent dissipation rates in a stirred tank using LDV with integral length scale, l_e, slightly higher than that used by Kresta and Wood (1993). Boffetta and Romano (2002) measured turbulent dissipation rate as a function of Reynolds number using a forward LDV and the mean normalized energy dissipation was found to be independent of Reynolds number.

Direct determination of energy dissipation in stirred vessels was achieved using two-point four-channel LDV, with nine out of the 12 mean squared velocity gradients were directly measured to calculate the dissipation rate (Ducci and Yianneskis, 2005). Probe arrangement of two-point LDV to measure the velocity gradients are shown in Fig. 4(b). The arrangements of probes allowed the measurements of the gradients $(\partial u_1/\partial x_1)^2$, $(\partial u_1/\partial x_3)^2$, $(\partial u_3/\partial x_3)^2$ and $(\partial u_3/\partial x_1)^2$. The maximum turbulent dissipation rate was found to vary by at least 30 percent, which was affected by the number of directly measured terms. The flow was found to deviate by up to 80 percent from local isotropy conditions. Therefore, the turbulent dissipation rate estimated from dimensional methods could be underestimated by around 40 percent. La Forgia et al. (2019) used LDV with two pairs of laser beams to get two velocity directions, stream-wise and normal to the baffled walls, for the estimation of turbulent dissipation rate in a rectangular channel. Time series of velocity were transformed, applying Taylor's frozen hypothesis, into a spatial velocity field required for the calculation of two-point correlation, where the velocity autocorrelation function, the second-order structure function and the third-order structure function were calculated. Different methods have been compared in the accuracy of estimating the dissipation rate and better accuracy was obtained using the second-order structure function with the Kolmogorov two-third law.

Al-Homoud and Hondzo (2007) compared LDV and PIV in the measurements of turbulent dissipation rate in an oscillating grid

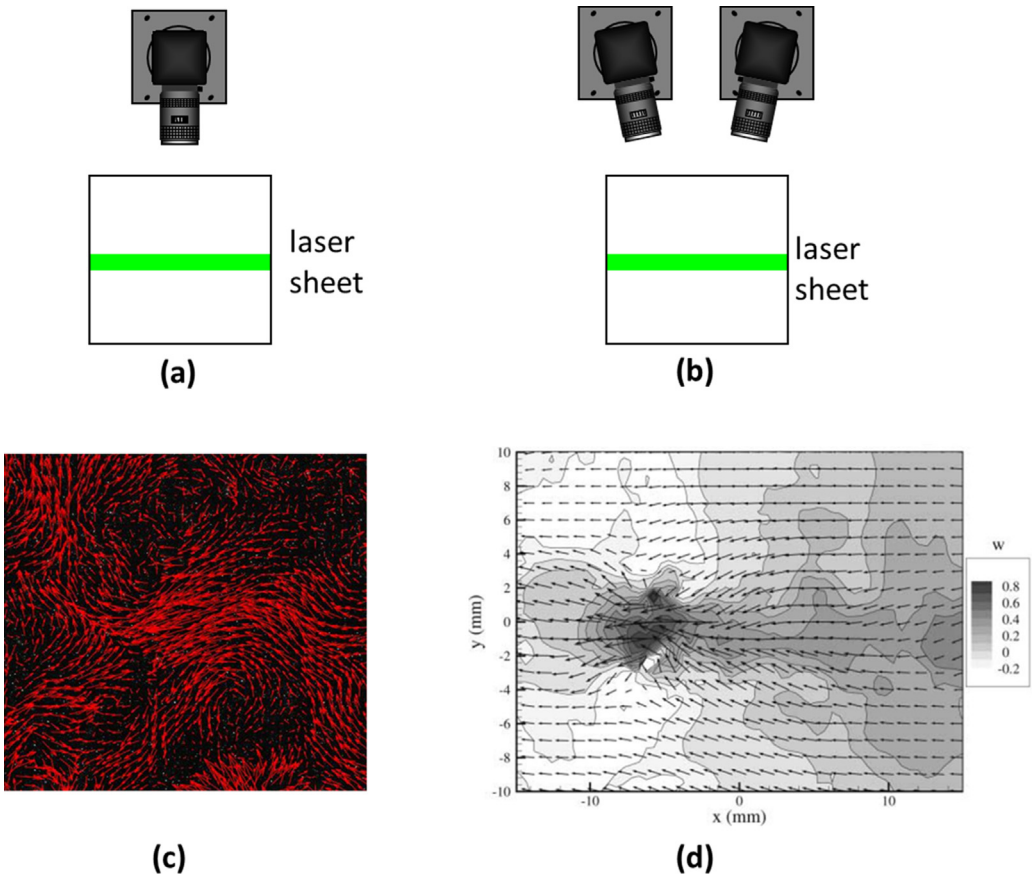

Fig. 5. (a) 2D PIV configuration (b) Stereo PIV configuration (c) Sample of two dimensional velocity field (d) Sample instantaneous stereo velocity with contours indicating the out-of-plane component of velocity (Hill et al., 2000).

turbulence. The estimated Eulerian frequency spectrum of LDV measurements was compared to theoretical functional relation for the estimation of turbulent dissipation rates using inertial dissipation method. PIV was used for a direct estimation of dissipation by evaluating spatially distributed velocity gradients. It is apparent that PIV could measure the fields of turbulent dissipation rate, whereas LDV is a point-based measurement technique with high temporal resolution. De Jong et al. (2009) characterized turbulent dissipation rate using a two-velocity-component LDV in addition to PIV. LDV measurements could provide a priori selection of optical PIV parameters and validate the PIV measurements. LDV measurements have also been used to validate the distribution of turbulent dissipation rate obtained from CFD predictions (Ng and Yianneskis, 2000).

4.3. Particle image velocimetry

It is worth noticing that the PIV method is a widely-accepted technique to measure flow field and the correlation method is generally used in PIV processing to calculate the spatially-averaged displacements of particle groups between images (Adrian, 1991). Most studies have used 2-D velocity fields and very few studies used stereo-PIV to estimate local or mean turbulent dissipation rates. A comparison of 2-D PIV and stereo-PIV is shown in Fig. 5. Sharp et al. (2000) measured turbulent dissipation in a stirred tank using PIV. Two methods, one using only one of the velocity gradient components and the other using all known components, were compared in the calculation of turbulent dissipation rates. The estimate using only one velocity gradient gave higher values than the estimate from all known components. The dissipation rate estimates from PIV measurements were compared to the previous studies using LDV method and the results were found in the range of the reported estimates. The author pointed out the limitations of the spatial resolution of velocity measurements using PIV. This was also confirmed by Saarenrinne and Piirto (2000) that the spatial resolution was a critical factor in the accuracy of the computed dissipation rate. Nevertheless, PIV can only resolve to a certain minimum length scale as the International PIV Challenge failed to exhibit high-spatial resolution due to the size of the interrogation area (Stanislas et al., 2008).

To mitigate the effects of low resolution on the estimation of turbulent dissipation rate, Sheng et al. (2000) employed a large-eddy PIV method to approximate the dissipation of energy at scales below the resolution of the measurements in a stirred tank. The turbulent dissipation rate was estimated from energy flux between the resolved and the sub-grid scales under dynamic equilibrium assumption. The Smagorinsky model was used to estimate the amount of dissipation rate contained in the unresolved scales and at least 70% of the true dissipation was captured (Sharp and Adrian, 2001). A large eddy simulation analogy was also used to estimate the dissipation rates calculated from three velocity components which were measured using stereo-PIV (Unadkat et al., 2011). Gabriele et al. (2011) used large eddy PIV to study the effect of particle loading on the modulation of turbulent dissipation rate in a stirred tank, The estimates of turbulent dissipation rate was found to decrease with increasing particle concentration. Mortensen et al. (2018) used a large-eddy 2D-PIV to investigate the effect of stator slot width on the local dissipation rate of

turbulent kinetic energy. A sub-resolution scale model was used to estimate local turbulent dissipation rate and wider slots were found to produce higher maximal turbulent dissipation rate.

Baldi and Yianneskis (2003, 2004) studied the effects of spatial resolution on the estimation of energy dissipation rate in stirred tanks. The dissipation was directly quantified from the fluctuating velocity gradient terms. In the impeller region of high turbulence, the Kolmogorov length scales were much smaller than the values in the bulk region. Lack of spatial resolution in the PIV measurements was the main reason for the inaccurate estimation of dissipation in the stirrer region. When the spatial resolution was three times the average Kolmogorov length scale in the tank, 90% of the true dissipation in the bulk flow and 65–70% of the true dissipation in the impeller stream can be determined.

Khan et al. (2006) applied a 'multi-block' method to improve the resolution of the measurements of stereo-PIV in a stirred tank with a 4-blade down-pumping pitched-blade turbine (PBT). It was found that around 44% of the total power was dissipated in the impeller region. It should be pointed out that most of the previous measurements gave ensemble-averaged results, and did not estimate instantaneous components of velocities. Micheletti et al. (2004) studied the spatial variations of the viscous dissipation of the turbulent energy by means of angle-resolved measurements. A significant variation of dissipation was found by three orders of magnitude from near the impeller to the bulk of the tank. The dissipation rate values were found to be concentrated in the vicinity of the trailing vortices and their distribution followed the path of the vortices across the tank.

The accuracy of turbulent dissipation rate measured by PIV is predominantly determined by the spatial resolution. The turbulent dissipation rate is undermeasured due to the filtering at low spatial resolution and it is overmeasured due to the amplification of noise by numerical differentiation of measured data (Tanaka and Eaton, 2007). When the noise in PIV measurements is assumed as a result of sub-pixel discrimination algorithm, a correction method was introduced to adjust the over measurement for high spatial resolution. It was suggested that the spatial resolution for PIV measurements of the dissipation rate should be in the range $\eta/10 < Dx < \eta/2$. Random error could lead to the overestimation of the turbulent dissipation rate when the velocity vector spacing is less than the Kolmogorov length scale. This problem could be mitigated by applying an efficient filtering procedure to downplay the effects of noise (Zaripov et al., 2019). Special attention should be payed to the strategy of filtering so that random noises, instead of real velocity fluctuations, are removed.

Most studies of turbulent dissipation rate were estimated based on two-dimensional velocity fields where only four velocity gradient terms could be extracted. The assumptions of isotropic or locally axisymmetric turbulence were made so that turbulent dissipation rate could be estimated from single or four velocity gradients. Gabriele et al. (2009) studied the local specific energy dissipation rates in a stirred tank with up- or down-pumping pitched blade turbine with angle resolved PIV. Three methodologies, direct calculation from fluctuating velocity gradients, dimensional analysis and Smagorinsky closure method to model unresolved length scales, were compared to estimate the local specific energy dissipation rate. Integrations of the total measured specific energy dissipation rates were compared to the power input in the PIV interrogated region of the tank. It was found that values from direct calculation method gave 20% of the total value whilst the dimensional analysis and Smagorinsky model methods overestimated it respectively by a factor of 5 and 2. Though the Smagorinsky model method gave more realistic result, the prediction depended considerably on the value of Smagorinsky constant. Delafosse et al. (2011) studied the effect of spatial resolution on the direct measurement of local dissipation rate. The spatial resolution should be of the same order of the Kolmogorov scale to ensure an accurate calculation of the turbulent dissipation rate. The measured dissipation rate corresponded to 90% of the exact value when the spatial resolution is around two times Kolmogorov scale. Hoque et al. (2015) also compared different methods of estimating energy dissipation rate. The method of direct calculation from fluctuating velocity gradients was found to under predict dissipation significantly due to the absence of spatial resolution of velocity gradient. To conclude, spatial resolution is a critical factor in the accuracy of the direct calculation of dissipation rate.

With the development of PIV technique, efforts have been devoted to, on the one hand, increasing the spatial and temporal resolution, and on the other hand achieving three dimensional PIV measurements. This paves the way to calculate turbulent dissipation rate directly from all instantaneous 3D velocity gradients without any simplifications or assumptions. More complex PIV setups have been explored to obtain 3-D, 3-C velocity field within the measurement volume. Zeff et al. (2003) measured the three components of velocity and all nine velocity gradients within a small volume using a 3D PIV. The turbulent dissipation rate was directly calculated from measured velocity gradients. Three laser sheets were aligned with the three sheets crossing at one vertex of the cube, which is shown in Fig. 6(a), in a way that each sheet illuminated one face of a small cubic volume. Three high-speed video cameras focused respectively on each sheet, recording the movements of fluorescent seeding particles in the sheet. It should be pointed out that the reconstruction of the 3D flow from these three

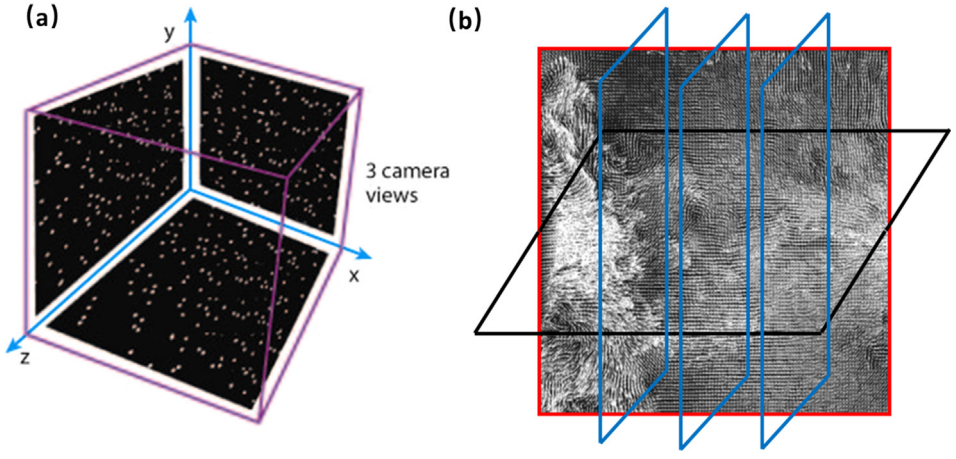

Fig. 6. (a) The contiguous faces of the measurement cube (Wallace and Vukoslavčević, 2010) (b) Five measurement planes (adapted from (Huchet et al., 2009)).

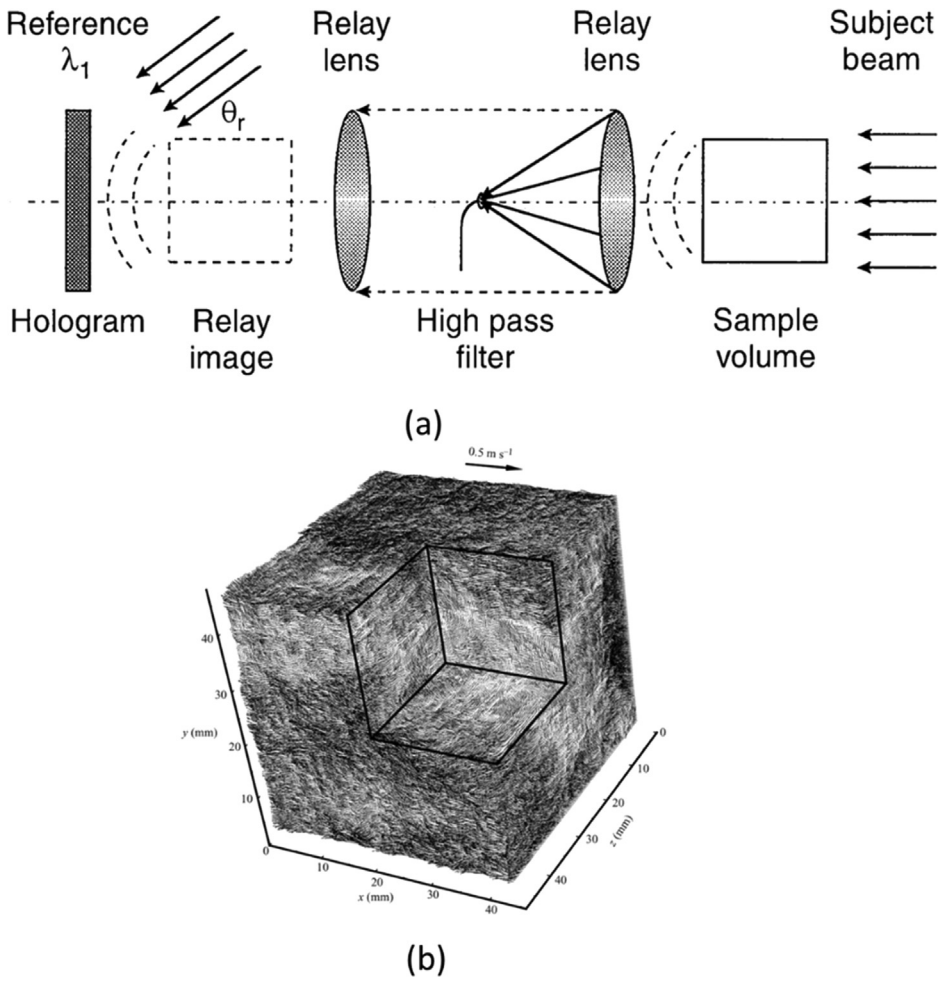

Fig. 7. (a) Principles of the hybrid HPIV system with solid rays indicating undisturbed subject beam and dashed rays and arcs denoting scattered light from particles (Zhang et al., 1997) (b) A sample three-dimensional, instantaneous velocity distribution in a turbulent duct flow measured by HPIV (Tao et al., 2002).

slices was based on the premise that the test volume was sufficiently small so that the flow within was locally linear. Similar experimental setup was used by Huchet et al. (2009) to directly measure the local kinetic energy dissipation rate without any simplifications made on the local isotropy of the turbulence. All spatial gradients of the fluctuating velocity components were directly measured as experiments were measured in three orthogonal planes using time-resolved 2D-PIV. Five measurement planes, as is shown in Fig. 6(b), have been used for the determination of the 12 components of the turbulent dissipation rate. Contributions from each plane to the measurement of dissipation were quantified. It was found that each contribution was approximately identical and roughly equaled half the total dissipation rate of turbulent kinetic energy.

Though the studies of using holography PIV have been limited due to is complexity, it could achieve three-dimensional velocity vector field using PTV algorithm. A hybrid holographic PIV system, as is shown in Fig. 7, has been developed for the measurement of instantaneous 3-D velocity distribution in turbulent flows (Tao et al., 2000; Zhang et al., 1997). It records the light scattered by the seeding particles and a reference beam, with the shape and location of the particles embedded in the interference patterns. Subgrid-scale dissipation was estimated from three-dimensional velocity measured at a high spatial resolution using holographic PIV (Tao et al., 2002). It was found that high positive sub-grid scale (SGS) dissipation occurred preferentially in regions with axisymmetric extending strain-rate and stress topologies, whilst high negative SGS dissipation occurred preferentially in regions of axisymmetric contracting SGS stress topology.

Tomographic PIV is capable of measuring 3-D, 3-C velocity field based on the illumination, recording and reconstruction of tracer particles within a 3D measurement volume (Elsinga et al., 2006; Scarano, 2012). The working principle of tomographic PIV is shown in Fig. 8. With at least four cameras, 3-D velocity field is reconstructed from several simultaneous views of the illuminated particles as a light intensity distribution by means of optical tomography. Worth and Nickels (2011) used tomographic PIV to achieve time-resolved volumetric measurement of fine-scale coherent structures in a mixing tank. Turbulent dissipation intermittency was studied and regions of intense rotation and energy dissipation were found significantly correlated, with these intermittent events clustered in the periphery of larger scale vortices. The spatial resolution of measurements is affected by the concentration of particle tracers that can be dealt with by the tomographic reconstruction. Tokgoz et al. (2012) studied the turbulent dissipation rate in Taylor-Couette flow using tomographic PIV. The effects of spatial resolution on the estimation of turbulent dissipation rate were assessed and underestimation of the dissipation rates was evident for fully turbulent flows. To ensure a good estimation of turbulent dissipation rate, a vector spacing (a ratio of vector spacing to the Kolmogorov scale) in the range of 1.5–2 were required. The degree of underestimation increased with Reynolds numbers, which was a result of the lack of spatial resolution. Earl et al. (2013) evaluated the turbulent dissipation rate in an open

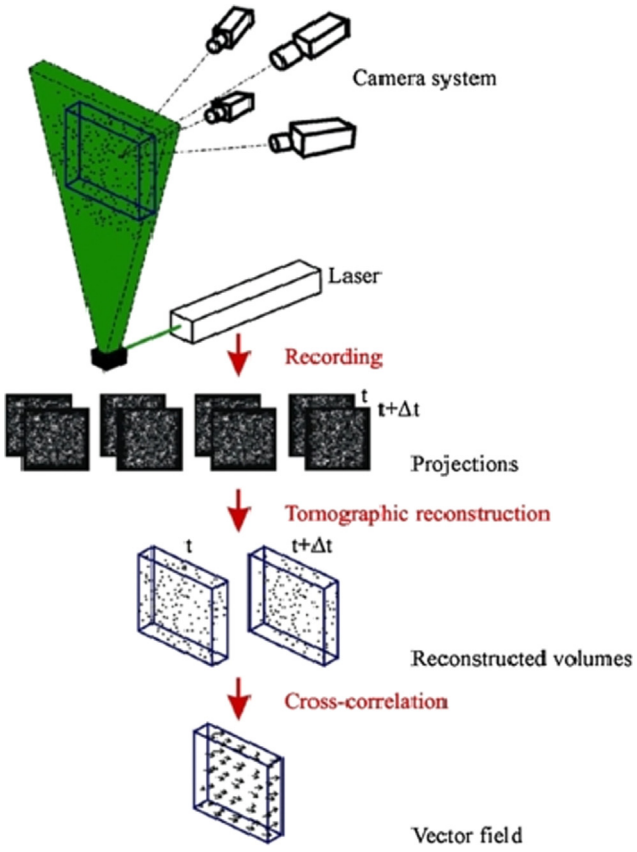

Fig. 8. Working principle of tomographic PIV (Scarano, 2012).

channel flow from tomographic PIV measurements. It was found that the measurement resolution was not fine enough to resolve the smallest Kolmogorov scales.

Due to the limitations embedded in the spatial resolution of PIV measurements, it is generally difficult to resolve down to the Kolmogorov scales. This is especially true for flows at high Reynolds number, where the size of the Kolmogorov length scale drops almost proportionally as the Reynolds number increases. Tanaka and Eaton (2010) achieved sub-Kolmogorov resolution PIV measurements of particle-laden forced turbulence using a 130 mm Cosmicar/Pentax extension in front of a 200 mm micro-Nikkor lens. Fiscaletti et al. (2014b) used long-range μPIV to resolve the small scales in a jet with a vector spacing of 1.5 times the size of the Kolmogorov length scale achieved. Though only 2D velocity fields were measured with axisymmetric assumption made about jet flow, the regions of intense dissipation were found to organize in the form of sheets with a characteristic thickness of approximately 10 times the size of the Kolmogorov length scale (10η). The regions of intense dissipation were highly correlated with the locations of intense vortices. This work demonstrated the suitability of long-range μPIV for characterizing turbulent flow structures at high Reynolds number. Fiscaletti et al. (2014a) further proposed using tomographic long-range microPIV to resolve the small-scale motions in the turbulent region of a jet at high Reynolds numbers. In this way, all velocity gradients could be measured to directly estimate the turbulent dissipation with adequate spatial resolution achieved.

4.4. Particle tracking velocimetry

Particle tracking velocimetry (PTV) is in common with PIV and it is often called low particle number density PIV (Adrian, 1991). In contrast to PIV where the mean displacement of a number of particles in an interrogation area is calculated, PTV tracks the trajectories of individual particles in three-dimensional space (Dracos, 1996). Mollet et al. (2004) used 3-dimensional particle tracking velocimetry (PTV) to estimate turbulent dissipation rate for the characterization of flow conditions acting on cells. 3-D trajectories of seeding particles were determined by using photogrammetric techniques and up to 1000 particles were tracked at a time. Therefore, PTV has modest spatial resolution as a result of the overlapping of particles when high particle concentrations are used, which was not sufficient to estimate local energy dissipation. A combination of adaptive Gaussian windows (AGW) and ensemble averaging (ES) was used to achieve high resolution of 3-D velocity fields. It was found in the bioreactor that the local dissipation in the impeller discharge region was found much higher than the mean dissipation, and the local dissipation could reach a value that result in the damage to animal cells.

The tracking of individual particles could refine the resolution of PIV measurements (Stitou and Riethmuller, 2001). Schneiders et al. (2017) used tomographic PTV and vortex-in-cell-plus to process the same tomographic PIV measurements for the purpose of improving spatial resolution. The vorticity and dissipation in a turbulent boundary layer estimated using tomogrtaphic PIV and the proposed method were compared to a DNS simulation. It was found that tomographic PIV underestimated the turbulent dissipation rate by approximately 50% and the newly proposed method gave a dissipation rate with less than 5% difference in comparison to the reference. At this stage, tomographic PIV is capable of measuring all the velocity gradients. Nevertheless, spatial resolution of tomographic PIV measurements is much less than that of the 2-D PIV measurements. It is demonstrated that the tomographic PTV and vortex-in-cell-plus method can be applied effectively to actual tomographic PIV for increased reconstruction quality of dissipation.

5. Estimating turbulent dissipation rate using DNS

Computational fluid dynamics have long been used to study turbulent dissipation rate and it is a huge topic by itself. We did not intend to include all such studies and only representative examples are discussed here. As direct numerical simulation (DNS) could resolve turbulence to the smallest scales, it is considered that turbulent dissipation rate calculated directly from the velocity field obtained from DNS predictions is most trustworthy. Therefore, DNS has been a versatile tool for the study of the properties of energy dissipation. DNS of homogeneous turbulence in a periodic box were carried out and it was found that the turbulent dissipation rate at high Reynolds numbers was independent of fluid viscosity (Sreenivasan, 1998). It was a constant of order unity when scaled on the integral scale and root-mean-square velocity. However, the value of constant was dependent on forcing at low wavenumbers. High-resolution DNS of a periodic box were performed and the normalized mean turbulent dissipation rate was shown to be independent of the fluid kinematic viscosity (Kaneda et al., 2003). Pearson et al. (2004) used DNS to study the dimensionless kinetic energy dissipation rate C_ε which appeared to change with time step due to the time lag between energy injection and energy dissipation. Rollin et al. (2011) showed that the high–Reynolds number value of the normalized dissipation rate depended on the shape of the low-wave-number forcing and that this shape dependence was captured by the upper-bound analysis.

Donzis et al. (2008) studied the effects of resolution on the turbulent dissipation in isotropic turbulence using DNS. The differences and similarities between dissipation and enstrophy were assessed and it was found that intense dissipation was likely to be accompanied by similarly intense enstrophy, but this was not necessarily true vice versa. Hamlington et al. (2012) studied the

local dissipation-scale distributions in turbulent channel flow using DNS. The dissipation-scale distributions and energy dissipation moments in the channel bulk flow agreed with those in homogeneous isotropic turbulence for sufficiently high Reynolds number. Different scenario was observed in the wall region and the authors speculated that this was caused by coherent vortices from the near-wall region. Due to the advantages of DNS for resolving dissipative scale vortices, results obtained from DNS have been used to evaluate different methods in the estimating of turbulent dissipation rate (Akinlabi et al., 2019). The superiority of DNS method is reflected by the fact that vortices of smallest scales are resolved so that turbulent dissipation are directly resolved. The major shortcomings of DNS are its extremely expensive computational cost and its capability of simulating only small regions.

Due to high computational cost of DNS, researchers prefer less computationally intensive methods, i.e. LES and RANS models, for the simulation of application cases. The deficiency of these methods is that eddies of Kolmogorov scales, which are responsible for energy dissipation, are not resolved. A large amount of work has been carried out using turbulence models, either Smagorinsky subgrid scale model or k-ε turbulence model, for the prediction of turbulent flows (Joshi et al., 2011, 2012). The dilemma is that less computationally cost methods have more assumptions or simplifications that may cost the accuracy of calculating the dissipation rate. Simulation results using LES method were compared to LDV or PIV measurements and a good balance between accuracy and computational cost was achieved (Delafosse et al., 2008; Hartmann et al., 2004; Soos et al., 2013). Special attention should be payed to the explanation of the distribution of turbulent dissipation rate. Though the distribution patterns of turbulent dissipation rate may be right, the values could be prejudiced due to the presumptions made in turbulence models.

6. Discussions

Experimental tools, including hot wire/film anemometry, LDV, PIV and PTV, have been widely applied to the measurements of turbulent flow fields for the characterization of local flow structures (Joshi et al., 2009). Each method has its strengths and weaknesses. They suffer from inherent limitations due to experimental conditions as well as limitations in the optical setup (De Jong et al., 2009). Hot wires have long been traditionally used to measure time series of velocities at a point though this technique is intrusive. Multiple probes could measure spatial components of velocity, but the interference from multiple probes presents a challenge to achieve reliable measurement of spatial and temporal components of velocities. Although LDV has high temporal resolution of velocity series, it is point-based measurement method and cannot predict the shape of the structures (Kresta and Wood, 1993). To date, the majority of the work has been applying PIV to measure planar flow field as it is capable of measuring spatial patterns and length scales of the structures. It should be mentioned that each experimental method suffers from their inherent limitations. Interestingly, turbulent dissipation rate is not a variable that can be measured directly from experiments and different methods could be used to quantify turbulent dissipation rate. Moreover, measurements using different experimental methods could be treated using different data processing methods to estimate turbulent dissipation rate. Therefore, the characteristics of experimental techniques should be discussed in accompanied with the characteristics of different data processing methods for a better estimation of turbulent dissipation rate.

Measurements using hot wires or LDV are point-based and high temporal resolution could be achieved for time series of velocity. Under the assumptions of isotropy and Taylor's hypothesis for frozen turbulence, which relates spatial statistics to temporal statistics, the calculation of turbulent dissipation rate from velocity spatial derivatives could be transformed into the calculation of velocity temporal gradient as is shown in Eq. (5). Taylor's hypothesis is limited to the uniform flows with low levels of turbulence (Elsner and Elsner, 1996). This comes with the presumption that all turbulent vortices are conveyed by streamwise velocity without changes in their properties. It is not trivial to connect the mean streamwise velocity to the small vortex structures. In some cases, likewise homogeneous isotropic turbulence where mean velocity is zero, this method is not applicable. A more general method is to measure velocity gradients which can be calculated from simultaneous measurements of velocities at two or more close points when two or more hot wires are used (Wallace and Vukoslavčević, 2010). Moreover, two-point LDV has been used to measure velocity gradients in a plane for the estimation of turbulent dissipation rate (Ducci and Yianneskis, 2005) and up to date LDV could achieve the measurement of complete velocity gradients in space. In most cases, likewise in a stirred tank, turbulent flow is far from homogeneous with turbulence in the stirrer region much higher than that in the bulk volume as is shown in Fig. 9(a). Therefore, multiple measurements should be carried out using LDV to estimate turbulent dissipation rates at different locations as is shown in Fig. 9(b). PIV is the technique that is capable of simultaneously measuring the distributions of turbulent dissipation rates.

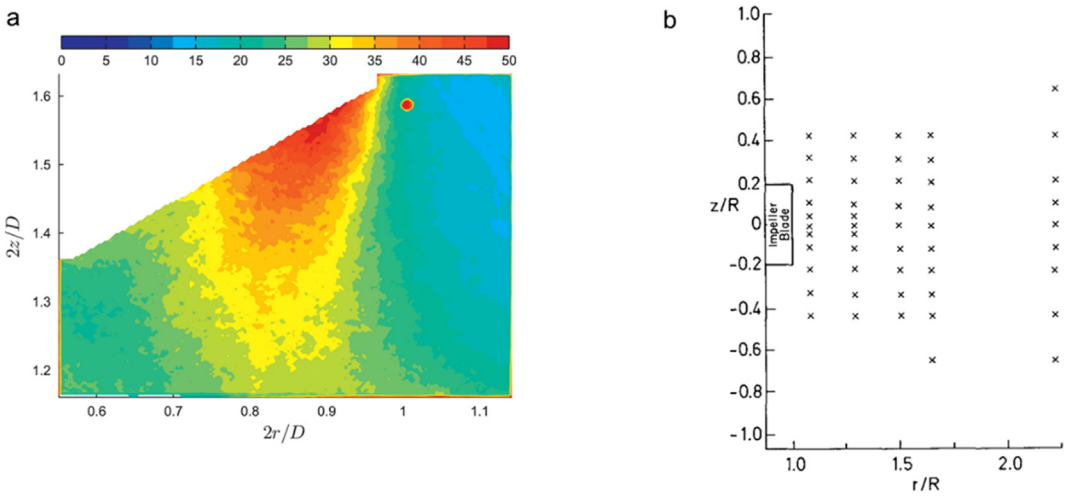

Fig. 9. (a) Contour of the turbulent dissipation rate from 2D-PIV measurements (Delafosse et al., 2011); (b) Locations of measurement points in and near the impeller stream for LDV measurements (Wu et al., 1989).

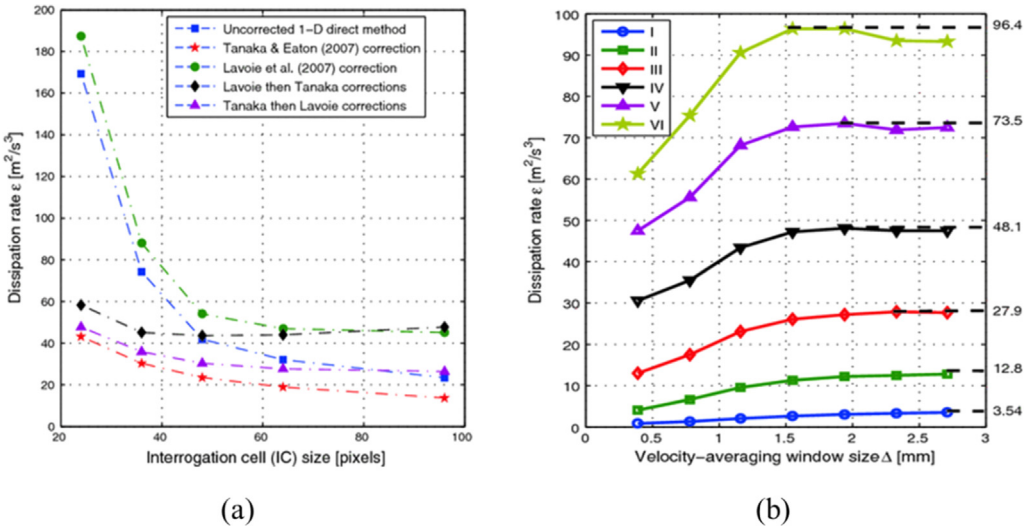

Fig. 10. (a) Effect of varying the interrogation cell size during analysis of the PIV images on the estimate of the dissipation rate; (b) Dependence of the large-eddy-PIV estimated dissipation rate ε on the size of the velocity-averaging window Δ for the six flow conditions (De Jong et al., 2009).

Local turbulent dissipation rates could be calculated from velocity gradients with assumptions made on isotropy or axisymmetry. Measurements of 3D velocity fields could be obtained from PTV, holographic PIV and tomographic PIV, but the spatial resolution of tomographic PIV measurements is much less than that of typical 2-D PIV measurements.

To strictly calculate turbulent dissipation rate from its definition, complete velocity derivatives are required to remove any assumptions or simplifications. Turbulent dissipation rate is a function of second-order strain rate and it requires velocity field of high resolution. Spatial resolution is one of the most important characteristics that determines the accuracy of the estimation of turbulent dissipation rate. The spatial resolution of hot wire technique is limited due to the length of hot wires and the distance between two parallel hot wires. Moreover, the measurement using hot wire in the downstream is affected by the existence of the wire in the upstream. The spatial resolution of LDV is determined by the size of beam interference which is typically in the range of 100–1000 μm. Velocity spatial derivatives could be achieved from two-point LDV and simultaneous measurement of 3 velocity components could be carried out using 3D LDV. Ducci and Yianneskis (2005) considered that the direct measurement of the fluctuating velocity gradients using LDV was more appropriate to determine turbulent dissipation rate, considering the spatial and temporal resolutions of LDV and no necessity of using Taylor's hypothesis and local isotropy assumptions. The characteristic size of the measuring volume should be of the order of the Kolmogorov length scale to ensure spatial resolution sufficient for accurate correlation and turbulent dissipation rate measurement (Eriksson and Karlsson, 1995). Ducci and Yianneskis (2005) also considered the spatial resolution of turbulent flow field should be resolved down to the Kolmogorov scale for the directly accurate estimate of turbulent dissipation rate.

Spatial resolution is also crucial for PIV measurements in the estimation of turbulent dissipation rate. A cross-correlation algorithm is generally applied to interrogation cell of PIV images to calculate the displacements of a group of particles. Xu and Chen (2013) found that the direct estimate of turbulent dissipation rate decreased significantly as interrogation window size increased, which is shown in Fig. 10(a). Though we can reduce the size of interrogation cell to increase spatial resolution, the size of interrogation cell should be sufficiently large to contain 10–20 seeding particles. This dilemma results in the limitations of PIV measurement in spatial resolution. Saarenrinne et al. (2001) suggested two times Kolmogorov scale for the spatial resolution of velocities of PIV experiments to estimate approximately 90% of the true dissipation rate. Large eddy PIV is applied to eliminate the necessity of resolving down to Kolmogorov scales and Smagorinsky model was used for estimating the unresolved small scales for the estimation of turbulent dissipation rate (Sheng et al., 2000). In the large-eddy PIV method, the velocity-averaging window size Δ in Eq. (9) plays a critical role and the estimate of turbulent dissipation rate depends on Δ as is shown in Fig. 10(b). Though there is a great disparity over the choice of the value of Smagorinsky constant and in some cases it represents an adjustment parameter, large eddy PIV could deal with the deficiency of spatial resolution and provide an estimation of the distribution of turbulent dissipation rate.

It should be mentioned that other velocity processing methods for turbulent dissipation rate, i.e. dimensional analysis, structure function, energy spectrum and forced balance of the turbulent kinetic energy equation, could also deal with the lack of spatial resolution. The estimations of turbulent dissipation rate using structure function and energy spectrum methods are based on the scaling law of inertial range. The estimation of turbulent dissipation rate from dimensional analysis is a statistical description of turbulence characteristics. These methods could only provide temporal or spatial mean turbulent dissipation rate, and the distribution of instantaneous turbulent dissipation rate can be obtained from forced balance of turbulent kinetic energy equation, fluctuating velocity gradients and fluctuating velocity gradients at subgrid scale using velocity fields measured by PIV. Researchers have compared different methods in processing velocity information achieved from different experimental techniques. Ducci and Yianneskis (2005) compared the energy spectrum approach in the processing of velocity data obtained from hot wires and LDV. It was found that the spectrum approach was suitable for a continuous signal obtained with hot wires. De Jong et al. (2009) compared different methods, i.e. direct method, structure function fit, large-eddy PIV, scaling argument and spectral fitting, for estimating turbulent dissipation rate from PIV data. Significant variations were observed among the different methods and the large-eddy PIV method produced the highest estimates, whilst the scaling

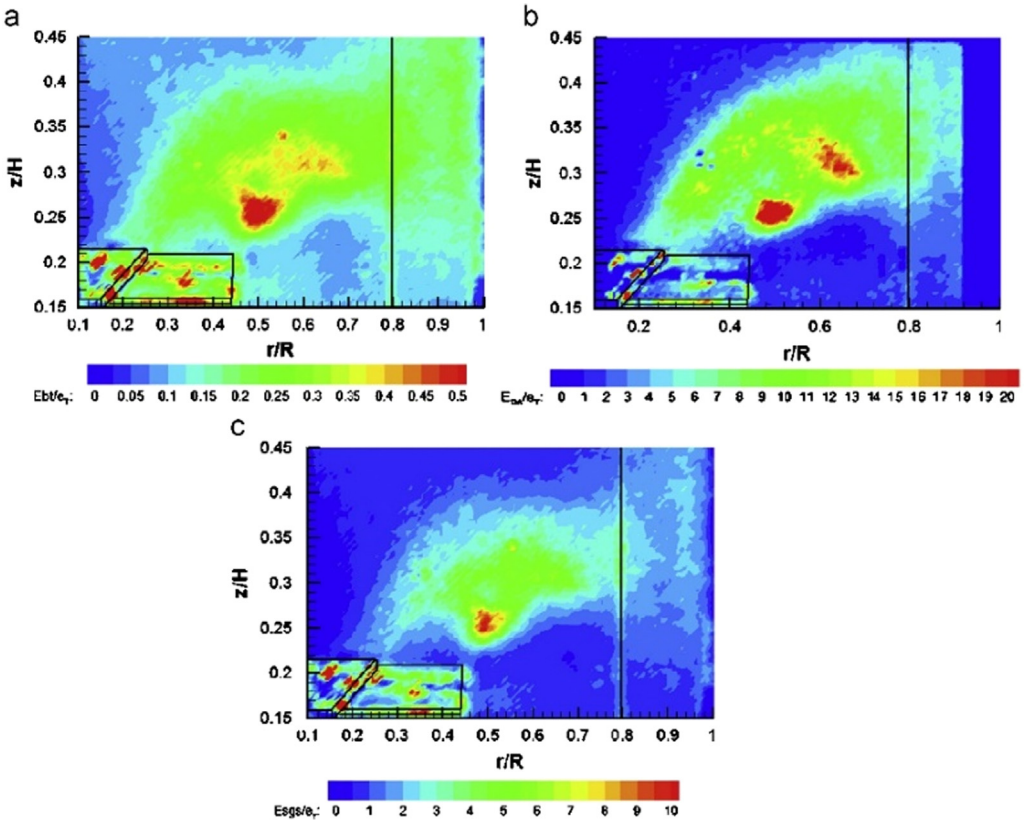

Fig. 11. Angle-resolved specific energy dissipation rates in the vicinity of the PBT-U impeller calculated using: (a) direct evaluation; (b) dimensional analysis; and (c) the SGS method (Gabriele et al., 2009).

argument method gave the lowest dissipation rate. Gabriele et al. (2009) compared direct method, Smagorinsky model and dimensional analysis in the estimate of local turbulent dissipation rate from PIV measurements. As is shown in Fig. 11, distribution patterns of turbulent dissipation rate were found similar using three different methodologies. It was suggested that only 5% was resolved using direct method which gave values one twentieth compared to Smagorinsky model. Dimensional analysis gave the highest values among the three methods. It is observed in the literature that results varied from work to work due to the assumptions made on the structure of turbulence and the limitations in the spatial or temporal resolutions in the experimental measurements.

It is worth noting that most studies of the measurements of turbulent dissipation rate is conducted in single phase turbulent flows. Measuring turbulent dissipation rate in multiphase systems is a huge topic by itself. It is more challenging than measurements in single phase turbulence for the reason that discrete phases will not only scatter laser light but also introduce flow structures of smaller scales. Due to the difficulties of achieving experimental measurements of multiphase flows using optical-based LDV and PIV methods, the report on the turbulent dissipation rate in multiphase flows is scarce. Moreover, it is still a controversial field with many controversial results on the modulation of the turbulent dissipation rate with adding a dispersed phase. Nevertheless, it is meaningful to measure the effects of dispersed phase on the distribution of turbulent dissipation rate, and vice versa, the effects of turbulent dissipation rate on the dynamics of the disperse phases as most industrial applications involve multiphase flows. The scarcity of reports on turbulent dissipation rate in multiphase flows points out the future directions of estimating turbulent dissipation rate.

7. Conclusions

Complete velocity gradient tensor is required to estimate turbulent dissipation rate strictly from its definition. As turbulent dissipation reflects the conversion of turbulent kinetic energy into heat through friction, it is necessary to resolve down to dissipative scale which is Kolmogorov scale. Current experimental techniques are capable of measuring the full velocity gradient tensor with reasonable accuracy and resolution and different calculation methods assume different assumptions on the structure of turbulence in the estimation of turbulent dissipation rate. This work has reviewed different experimental techniques, i.e. hot wires, LDV, PIV and PTV, in accompanied with different calculation methods, i.e. direct calculation using fluctuating velocity gradients, Smagorinsky closure method, dimensional analysis, structure function, energy spectrum and forced balance of the TKE equation, in the estimate of turbulent dissipation rate. It is identified that various assumptions are made in different calculation methods and there are limitations in the spatial or temporal resolutions of different experimental techniques. Taylor's hypothesis is applied to convert velocity temporal derivatives measured using one point-based hot wire or LDV to spatial derivatives. Though multipoint hot wire probes or LDV could achieve velocity spatial derivatives, measurement resolution can only decrease to certain dimension due to physical interference of multi probes or size of beam interference of LDV. Spatial resolution is also crucial for PIV measurements which are capable of simultaneously measuring the distribution of turbulent dissipation rate. Still, estimation of turbulent dissipation rate in turbulent multiphase flows is scarce. Future work in this area should aim to combine characteristics of experimental techniques with different calculation methods. Thus, estimation of turbulent dissipation rate can be predicted in a more

direct and accurate way using fundamental analysis of the inside physics with less dependency on empirical factors.

Declaration of Competing Interest

The authors declare that they have no known competing financial interests or personal relationships that could have appeared to influence the work reported in this paper.

Acknowledgements

We gratefully acknowledge that this work was supported by National Natural Science Foundation of China (NSFC grants 91852205, 91741101, and 11961131006), NSFC Basic Science Center Program (Award number 11988102), Guangdong Provincial Key Laboratory of Turbulence Research and Applications (2019B21203001), and Shenzhen Science and Technology Program (Grant No. KQTD20180411143441009) and by the U.S. National Science Foundation (NSF) under grants CNS1513031 and CBET-1706130. Computing resources are provided by the Center of Computational Science and Engineering at the Southern University of Science and Technology, and by National Center for Atmospheric Research through CISL-UDEL0001.

References

Adrian, R.J., 1991. Particle-imaging techniques for experimental fluid mechanics. Annu. Rev. Fluid Mech. 23, 261–304.
Akinlabi, E.O., Wacławczyk, M., Mellado, J.P., Malinowski, S.P., 2019. Estimating turbulence kinetic energy dissipation rates in the numerically simulated stratocumulus cloud-top mixing layer: evaluation of different methods. J. Atmos. Sci. 76, 1471–1488.
Al-Homoud, A., Hondzo, M., 2007. Energy dissipation estimates in oscillating grid setup: LDV and PIV measurements. Environ. Fluid Mech. 7, 143–158.
Aloi, L.E., Cherry, R.S., 1996. Cellular response to agitation characterized by energy dissipation at the impeller tip. Chem. Eng. Sci. 51, 1523–1529.
Antonia, R.A., 2003. On estimating mean and instantaneous turbulent energy dissipation rates with hot wires. Exp. Therm Fluid Sci. 27, 151–157.
Antonia, R.A., Kim, J., Browne, L.W.B., 2006. Some characteristics of small-scale turbulence in a turbulent duct flow. J. Fluid Mech. 233, 369–388.
Antonia, R.A., Pearson, B.R., 2000. Effect of initial conditions on the mean energy dissipation rate and the scaling exponent. Phys. Rev. E 62, 8086–8090.
Azad, R., Kassab, S., 1989. New method of obtaining dissipation. Exp. Fluids 7, 81–87.
Bailey, S., Witte, B., 2016. On the universality of local dissipation scales in turbulent channel flow. J. Fluid Mech. 786, 234–252.
Baldi, S., Yianneskis, M., 2003. On the direct measurement of turbulence energy dissipation in stirred vessels with PIV. Industr. Eng. Chem. Res. 42, 7006–7016.
Baldi, S., Yianneskis, M., 2004. On the quantification of energy dissipation in the impeller stream of a stirred vessel from fluctuating velocity gradient measurements. Chem. Eng. Sci. 59, 2659–2671.
Bałdyga, J., Pohorecki, R., 1995. Turbulent micromixing in chemical reactors—a review. Chem. Eng. J. Biochem. Eng. J. 58, 183–195.
Banakh, V., Smalikho, I., Falits, A., 2017. Estimation of the turbulence energy dissipation rate in the atmospheric boundary layer from measurements of the radial wind velocity by micropulse coherent Doppler lidar. Opt. Express 25, 22679–22692.
Banerjee, S., Scott, D.S., Rhodes, E., 1968. Mass transfer to falling wavy liquid films in turbulent flow. Industr. Eng. Chem. Fundam. 7, 22–27.
Batchelor, G.K., 1953. The Theory of Homogeneous Turbulence. Cambridge University Press.
Bertens, G., van der Voort, D., Bocanegra-Evans, H., van de Water, W., 2015. Large-eddy estimate of the turbulent dissipation rate using PIV. Exp. Fluids 56, 89.
Boffetta, G., Romano, G., 2002. Structure functions and energy dissipation dependence on Reynolds number. Phys. Fluids 14, 3453–3458.
Bos, W.J., Rubinstein, R., 2017. Dissipation in unsteady turbulence. Phys. Rev. Fluids 2, 022601.
Bos, W.J., Shao, L., Bertoglio, J.-P., 2007. Spectral imbalance and the normalized dissipation rate of turbulence. Phys. Fluids 19, 045101.
Browne, L., Antonia, R., Shah, D., 1987. Turbulent energy dissipation in a wake. J. Fluid Mech. 179, 307–326.
Burattini, P., Lavoie, P., Antonia, R.A., 2005. On the normalized turbulent energy dissipation rate. Phys. Fluids 17, 098103.
Calabrese, R., Stoots, C., 1989. Flow in the impeller region of a stirred tank. Chem. Eng. Prog. 85, 43–50.
Chen, S., Chen, X., Wan, D., Yi, X., Sun, X., Ji, L., Wang, G., 2019. A lattice Boltzmann study of the collisions in a particle-bubble system under turbulent flows. Powder Technol.
Choi, H., Moin, P., Kim, J., 1994. Active turbulence control for drag reduction in wall-bounded flows. J. Fluid Mech. 262, 75–110.
Cohn, S.A., 1995. Radar measurements of turbulent eddy dissipation rate in the troposphere: a comparison of techniques. J. Atmos. Oceanic Technol. 12, 85–95.
Costes, J., Couderc, J., 1988. Influence of the size of the units: I Mean flow and turbulence. Chem. Eng. Sci 43, 2751.
Crane, R.K., 1980. A review of radar observations of turbulence in the lower stratosphere. Radio Sci. 15, 177–193.
Czarske, J.W., 2006. Laser Doppler velocimetry using powerful solid-state light sources. Meas. Sci. Technol. 17, R71–R91.
Davies, J.T., 1985. Drop sizes of emulsions related to turbulent energy dissipation rates. Chem. Eng. Sci. 40, 839–842.
Davies, J.T., 2012. Turbulence Phenomena: An Introduction to the Eddy Transfer of Momentum, Mass, and Heat, Particularly at Interfaces. Elsevier.
De Jong, J., Cao, L., Woodward, S., Salazar, J., Collins, L., Meng, H., 2009. Dissipation rate estimation from PIV in zero-mean isotropic turbulence. Exp. Fluids 46, 499.
Delafosse, A., Collignon, M.-L., Crine, M., Toye, D., 2011. Estimation of the turbulent kinetic energy dissipation rate from 2D-PIV measurements in a vessel stirred by an axial Mixel TTP impeller. Chem. Eng. Sci. 66, 1728–1737.
Delafosse, A., Line, A., Morchain, J., Guiraud, P., 2008. LES and URANS simulations of hydrodynamics in mixing tank: comparison to PIV experiments. Chem. Eng. Res. Des. 86, 1322–1330.
Deshpande, S.S., Mathpati, C.S., Gulawani, S.S., Joshi, J.B., Ravi Kumar, V., 2009. Effect of flow structures on heat transfer in single and multiphase jet reactors. Industr. Eng. Chem. Res. 48, 9428–9440.
Doering, C.R., Constantin, P., 1992. Energy dissipation in shear driven turbulence. Phys. Rev. Lett. 69, 1648.
Doering, C.R., Foias, C., 2002. Energy dissipation in body-forced turbulence. J. Fluid Mech. 467, 289–306.
Donzis, D., Yeung, P., Sreenivasan, K., 2008. Dissipation and enstrophy in isotropic turbulence: resolution effects and scaling in direct numerical simulations. Phys. Fluids 20, 045108.
Dracos, T., 1996. Particle Tracking Velocimetry (PTV). In: Dracos, T. (Ed.), Three-Dimensional Velocity and Vorticity Measuring and Image Analysis Techniques: Lecture Notes from the Short Course held in Zürich, Switzerland, 3–6 September 1996. Springer, Netherlands, Dordrecht, pp. 155–160.
Ducci, A., Yianneskis, M., 2005. Direct determination of energy dissipation in stirred vessels with two-point LDA. AIChE J. 51, 2133–2149.
Earl, T.A., Cochard, S., Tremblais, B., Thomas, L., David, L., 2013. Evaluation of the energy dissipation from tomographic PIV measurements in an open channel flow behind regular grids. In: Proceedings of the 35th IAHR World Congress, September 8–13, Chengdu, China, pp. 1–8.
Elsinga, G.E., Scarano, F., Wieneke, B., van Oudheusden, B.W., 2006. Tomographic particle image velocimetry. Exp. Fluids 41, 933–947.
Elsner, J., Elsner, W., 1996. On the measurement of turbulence energy dissipation. Meas. Sci. Technol. 7, 1334.
Elsner, J.W., Domagala, P., Elsner, W., 1993. Effect of finite spatial resolution of hot-wire anemometry on measurements of turbulence energy dissipation. Meas. Sci. Technol. 4, 517–523.
Eriksson, J.G., Karlsson, R.I., 1995. An investigation of the spatial resolution requirements for two-point correlation measurements using LDV. Exp. Fluids 18, 393–396.
Escudié, R., Liné, A., 2003. Experimental analysis of hydrodynamics in a radially agitated tank. AIChE J. 49, 585–603.
Fiscaletti, D., Overmars, E., Westerweel, J., Elsinga, G., 2014a. Tomographic long-range microPIV to resolve the small-scale motions in the turbulent region of a jet at high Reynolds numbers. In: 17th int. symposium on application of laser techniques to fluid mechanics. Lisbon, Portugal.
Fiscaletti, D., Westerweel, J., Elsinga, G., 2014b. Long-range μPIV to resolve the small scales in a jet at high Reynolds number. Exp. Fluids 55, 1812.
Gabriele, A., Nienow, A., Simmons, M., 2009. Use of angle resolved PIV to estimate local specific energy dissipation rates for up-and down-pumping pitched blade agitators in a stirred tank. Chem. Eng. Sci. 64, 126–143.
Gabriele, A., Tsoligkas, A., Kings, I., Simmons, M., 2011. Use of PIV to measure turbulence modulation in a high throughput stirred vessel with the addition of high Stokes number particles for both up-and down-pumping configurations. Chem. Eng. Sci. 66, 5862–5874.
Ganapathisubramani, B., Lakshminarasimhan, K., Clemens, N.T., 2007. Determination of complete velocity gradient tensor by using cinematographic stereoscopic PIV in a turbulent jet. Exp. Fluids 42, 923–939.
Ganapathisubramani, B., Lakshminarasimhan, K., Clemens, N.T., 2008. Investigation of three-dimensional structure of fine scales in a turbulent jet by using cinematographic stereoscopic particle image velocimetry. J. Fluid Mech. 598, 141–175.
George, W.K., Hussein, H.J., 2006. Locally axisymmetric turbulence. J. Fluid Mech. 233, 1–23.
Gollub, J.P., Clarke, J., Gharib, M., Lane, B., Mesquita, O., 1991. Fluctuations and transport in a stirred fluid with a mean gradient. Phys. Rev. Lett. 67, 3507.
Goto, S., Vassilicos, J.C., 2009. The dissipation rate coefficient of turbulence is not universal and depends on the internal stagnation point structure. Phys. Fluids 21, 035104.
Hamlington, P.E., Krasnov, D., Boeck, T., Schumacher, J., 2012. Local dissipation scales and energy dissipation-rate moments in channel flow. J. Fluid Mech. 701, 419–429.

Hartmann, H., Derksen, J., Montavon, C., Pearson, J., Hamill, I., Van den Akker, H., 2004. Assessment of large eddy and RANS stirred tank simulations by means of LDA. Chem. Eng. Sci. 59, 2419–2432.
Hearst, R.J., Lavoie, P., 2014. Decay of turbulence generated by a square-fractal-element grid. J. Fluid Mech. 741, 567–584.
Hermawan, E., Tsuda, T., 1999. Estimation of turbulence energy dissipation rate and vertical eddy diffusivity with the MU radar RASS. J. Atmos. Solar-Terrestrial Phys. 61, 1123–1130.
Hill, D.F., Sharp, K.V., Adrian, R.J., 2000. Stereoscopic particle image velocimetry measurements of the flow around a Rushton turbine. Exp. Fluids 29, 478–485.
Hinze, J.O., 1975. Turbulence. McGraw-Hill.
Hocking, W.K., 1985. Measurement of turbulent energy dissipation rates in the middle atmosphere by radar techniques: a review. Radio Sci. 20, 1403–1422.
Hoque, M.M., Sathe, M.J., Mitra, S., Joshi, J.B., Evans, G.M., 2015. Comparison of specific energy dissipation rate calculation methodologies utilising 2D PIV velocity measurement. Chem. Eng. Sci. 137, 752–767.
Huchet, F., Line, A., Morchain, J., 2009. Evaluation of local kinetic energy dissipation rate in the impeller stream of a Rushton turbine by time-resolved PIV. Chem. Eng. Res. Des. 87, 369–376.
Hwang, W., Eaton, J., 2004. Creating homogeneous and isotropic turbulence without a mean flow. Exp. Fluids 36, 444–454.
Isaza, J.C., Salazar, R., Warhaft, Z., 2014. On grid-generated turbulence in the near- and far field regions. J. Fluid Mech. 753, 402–426.
Joshi, J.B., Nere, N.K., Rane, C.V., Murthy, B., Mathpati, C.S., Patwardhan, A.W., Ranade, V.V., 2011. CFD simulation of stirred tanks: comparison of turbulence models. Part I: radial flow impellers. Can. J. Chem. Eng. 89, 23–82.
Joshi, J.B., Nere, N.K., Rane, C.V., Murthy, B.N., Mathpati, C.S., Patwardhan, A.W., Ranade, V.V., 2012. CFD simulation of stirred tanks: comparison of turbulence models (Part II: Axial flow impellers, multiple impellers and multiphase dispersions). Can. J. Chem. Eng. 89, 754–816.
Joshi, J.B., Tabib, M.V., Deshpande, S.S., Mathpati, C.S., 2009. Dynamics of flow structures and transport phenomena, 1. Experimental and numerical techniques for identification and energy content of flow structures. Indust. Eng. Chem. Res. 48, 8244–8284.
Kader, B., Yaglom, A., 1972. Heat and mass transfer laws for fully turbulent wall flows. Int. J. Heat Mass Transfer 15, 2329–2351.
Kaneda, Y., Ishihara, T., Yokokawa, M., Itakura, K.I., Uno, A., 2003. Energy dissipation rate and energy spectrum in high resolution direct numerical simulations of turbulence in a periodic box. Phys. Fluids 15, L21–L24.
Khan, F., Rielly, C., Brown, D., 2006. Angle-resolved stereo-PIV measurements close to a down-pumping pitched-blade turbine. Chem. Eng. Sci. 61, 2799–2806.
Kohma, M., Sato, K., Tomikawa, Y., Nishimura, K., Sato, T., 2019. Estimate of turbulent energy dissipation rate from the VHF radar and radiosonde observations in the Antarctic. J. Geophys. Res.: Atmos. 124, 2976–2993.
Kolmogorov, A.N., 1941a. Dissipation of energy in locally isotropic turbulence, Akademiia Nauk SSSR Doklady, p. 16.
Kolmogorov, A.N., 1941b. The local structure of turbulence in incompressible viscous fluid for very large Reynolds number. Dokl. Akad. Nauk SSSR 30, 301–305.
Kolmogorov, A.N., 1941c. On degeneration (decay) of isotropic turbulence in an incompressible viscous liquid. Dokl. Akad. Nauk SSSR, 538–540.
Kolmogorov, A.N., 1962. A refinement of previous hypotheses concerning the local structure of turbulence in a viscous incompressible fluid at high Reynolds number. J. Fluid Mech. 13, 82–85.
Kresta, S.M., Wood, P.E., 1991. Prediction of the three-dimensional turbulent flow in stirred tanks. AlChE J. 37, 448–460.
Kresta, S.M., Wood, P.E., 1993. The flow field produced by a pitched blade turbine: characterization of the turbulence and estimation of the dissipation rate. Chem. Eng. Sci. 48, 1761–1774.
Kuzzay, D., Faranda, D., Dubrulle, B., 2015. Global vs local energy dissipation: The energy cycle of the turbulent von Kármán flow. Phys. Fluids 27, 075105.
La Forgia, N., Herø, E.H., Solsvik, J., Jakobsen, H.A., 2019. Dissipation rate estimation in a rectangular shaped test section with periodic structure at the walls. Chem. Eng. Sci. 195, 159–178.
Lamont, J.C., Scott, D., 1970. An eddy cell model of mass transfer into the surface of a turbulent liquid. AlChE J. 16, 513–519.
Lawn, C., 1971. The determination of the rate of dissipation in turbulent pipe flow. J. Fluid Mech. 48, 477–505.
Lekakis, I., 1996. Calibration and signal interpretation for single and multiple hot-wire/hot-film probes. Meas. Sci. Technol. 7, 1313–1333.
Liu, S., Meneveau, C., Katz, J., 1994. On the properties of similarity subgrid-scale models as deduced from measurements in a turbulent jet. J. Fluid Mech. 275, 83–119.
Luo, H., Svendsen, H.F., 1996. Theoretical model for drop and bubble breakup in turbulent dispersions. AlChE J. 42, 1225–1233.
McComb, W., Berera, A., Yoffe, S., Linkmann, M., 2015. Energy transfer and dissipation in forced isotropic turbulence. Physical Review E 91, 043013.
Meneveau, C., Sreenivasan, K., 1991. The multifractal nature of turbulent energy dissipation. J. Fluid Mech. 224, 429–484.
Meyers, J., Sagaut, P., 2006. On the model coefficients for the standard and the variational multi-scale Smagorinsky model. J. Fluid Mech. 569, 287–319.
Micheletti, M., Baldi, S., Yeoh, S., Ducci, A., Papadakis, G., Lee, K., Yianneskis, M., 2004. On spatial and temporal variations and estimates of energy dissipation in stirred reactors. Chem. Eng. Res. Des. 82, 1188–1198.
Mollet, M., Ma, N., Zhao, Y., Brodkey, R., Taticek, R., Chalmers, J.J., 2004. Bioprocess equipment: characterization of energy dissipation rate and its potential to damage cells. Biotechnol. Progr. 20, 1437–1448.
Morshed, K.N., Venayagamoorthy, S.K., Dasi, L.P., 2013. Intermittency and local dissipation scales under strong mean shear. Phys. Fluids 25, 011701.
Mortensen, H.H., Innings, F., Håkansson, A., 2018. Local levels of dissipation rate of turbulent kinetic energy in a rotor–stator mixer with different stator slot widths—an experimental investigation. Chem. Eng. Res. Des. 130, 52–62.
Mouri, H., Hori, A., Kawashima, Y., Hashimoto, K., 2012. Large-scale length that determines the mean rate of energy dissipation in turbulence. Phys. Rev. E 86, 026309.
Nagata, K., Sakai, Y., Inaba, T., Suzuki, H., Terashima, O., Suzuki, H., 2013. Turbulence structure and turbulence kinetic energy transport in multiscale/fractal-generated turbulence. Phys. Fluids 25, 065102.
Ng, K., Yianneskis, M., 2000. Observations on the distribution of energy dissipation in stirred vessels. Chem. Eng. Res. Des. 78, 334–341.
Nguyen, A.V., An-Vo, D.-A., Tran-Cong, T., Evans, G.M., 2016. A review of stochastic description of the turbulence effect on bubble-particle interactions in flotation. Int. J. Miner. Process. 156, 75–86.
Pearson, B.R., Krogstad, PC.-Å., Water, W.V.D., 2002. Measurements of the turbulent energy dissipation rate. Phys. Fluids 14, 1288–1290.
Pearson, B.R., Yousef, T.A., Haugen, N.E.L., Brandenburg, A., Krogstad, P.-Å., 2004. Delayed correlation between turbulent energy injection and dissipation. Phys. Rev. E 70, 056301.
Pope, S.B., 2001. Turbulent Flows. IOP Publishing.
Prince, M.J., Blanch, H.W., 1990. Bubble coalescence and break-up in air-sparged bubble columns. AlChE J. 36, 1485–1499.
Puga, A.J., LaRue, J.C., 2017. Normalized dissipation rate in a moderate Taylor Reynolds number flow. J. Fluid Mech. 818, 184–204.
Richardson, L.F., 2007. Weather Prediction by Numerical Process. Cambridge University Press.
Rollin, B., Dubief, Y., Doering, C., 2011. Variations on Kolmogorov flow: turbulent energy dissipation and mean flow profiles. J. Fluid Mech. 670, 204–213.
Ross, T., Lueck, R., 2005. Estimating turbulent dissipation rates from acoustic backscatter. Deep Sea Res. Part I: Oceanogr. Res. Papers 52, 2353–2365.
Saarenrinne, P., Piirto, M., 2000. Turbulent kinetic energy dissipation rate estimation from PIV velocity vector fields. Exp. Fluids 29, S300–S307.
Saarenrinne, P., Piirto, M., Eloranta, H., 2001. Experiences of turbulence measurement with PIV. Meas. Sci. Technol. 12, 1904.
Sajjadi, B., Raman, A.A.A., Shah, R.S.S.R.E., Ibrahim, S., 2013. Review on applicable breakup/coalescence models in turbulent liquid-liquid flows. Rev. Chem. Eng. 29, 131–158.
Saw, E.-W., Kuzzay, D., Faranda, D., Guittonneau, A., Daviaud, F., Wiertel-Gasquet, C., Padilla, V., Dubrulle, B., 2016. Experimental characterization of extreme events of inertial dissipation in a turbulent swirling flow. Nat. Commun. 7, 12466.
Scarano, F., 2012. Tomographic PIV: principles and practice. Meas. Sci. Technol. 24, 012001.
Schacher, G., Davidson, K., Houlihan, T., Fairall, C., 1981. Measurements of the rate of dissipation of turbulent kinetic energy, ε, over the ocean. Boundary-Layer Meteorol. 20, 321–330.
Schäfer, M., Höfken, M., Durst, F., 1997. Detailed LDV measurements for visualization of the flow field within a stirred-tank reactor equipped with a Rushton turbine. Chem. Eng. Res. Des. 75, 729–736.
Schneiders, J.F., Scarano, F., Elsinga, G.E., 2017. Resolving vorticity and dissipation in a turbulent boundary layer by tomographic PTV and VIC+. Exp. Fluids 58, 27.
Schumacher, J., 2007. Sub-Kolmogorov-scale fluctuations in fluid turbulence. EPL (Europhys. Lett.) 80, 54001.
Seoud, R.E., Vassilicos, J.C., 2007. Dissipation and decay of fractal-generated turbulence. Phys. Fluids 19, 105108.
Sharp, K., Adrian, R., 2001. PIV study of small-scale flow structure around a Rushton turbine. AlChE J. 47, 766–778.
Sharp, K.V., Kim, K.C., Adrian, R., 2000. Dissipation estimation around a Rushton turbine using particle image velocimetry, Laser Techniques Applied to Fluid Mechanics. Springer, pp. 337–354.
Sheng, J., Meng, H., Fox, R., 2000. A large eddy PIV method for turbulence dissipation rate estimation. Chem. Eng. Sci. 55, 4423–4434.
Soos, M., Kaufmann, R., Winteler, R., Kroupa, M., Lüthi, B., 2013. Determination of maximum turbulent energy dissipation rate generated by a rushton impeller through large eddy simulation. AlChE J. 59, 3642–3658.
Sreenivasan, K.R., 1984. On the scaling of the turbulence energy dissipation rate. Phys. Fluids 27, 1048–1051.
Sreenivasan, K.R., 1995. On the universality of the Kolmogorov constant. Phys. Fluids 7, 2778–2784.
Sreenivasan, K.R., 1998. An update on the energy dissipation rate in isotropic turbulence. Phys. Fluids 10, 528–529.
Sreenivasan, K.R., Antonia, R.A., 1997. The phenomenology of small-scale turbulence. Annu. Rev. Fluid Mech. 29, 435–472.
Stanislas, M., Okamoto, K., Kähler, C.J., Westerweel, J., Scarano, F., 2008. Main results of the third international PIV challenge. Exp. Fluids 45, 27–71.
Stitou, A., Riethmuller, M.L., 2001. Extension of PIV to super resolution using PTV. Meas. Sci. Technol. 12, 1398–1403.
Tanaka, T., Eaton, J.K., 2007. A correction method for measuring turbulence kinetic energy dissipation rate by PIV. Exp. Fluids 42, 893–902.
Tanaka, T., Eaton, J.K., 2010. Sub-Kolmogorov resolution partical image velocimetry measurements of particle-laden forced turbulence. J. Fluid Mech. 643, 177–206.

Tao, B., Katz, J., Meneveau, C., 2000. Geometry and scale relationships in high Reynolds number turbulence determined from three-dimensional holographic velocimetry. Phys. Fluids 12, 941–944.
Tao, B., Katz, J., Meneveau, C., 2002. Statistical geometry of subgrid-scale stresses determined from holographic particle image velocimetry measurements. J. Fluid Mech. 457, 35–78.
Taylor, G.I., 1935. Statistical theory of turbulence IV-diffusion in a turbulent air stream. Proc. R. Soc. Lond. Series A-Math. Phys. Sci. 151, 465–478.
Taylor, G.I., 1938. The spectrum of turbulence. Proc. R. Soc. Lond.. Series A-Math. Phys. Sci. 164, 476–490.
Tennekes, H., Lumley, J.L., Lumley, J., 1972. A First Course in Turbulence. MIT press.
Tokgoz, S., Elsinga, G.E., Delfos, R., Westerweel, J., 2012. Spatial resolution and dissipation rate estimation in Taylor-Couette flow for tomographic PIV. Exp. Fluids 53, 561–583.
Tropea, C., 1995. Laser Doppler anemometry: recent developments and future challenges. Meas. Sci. Technol. 6, 605.
Tsinober, A., Kit, E., Dracos, T., 1992. Experimental investigation of the field of velocity gradients in turbulent flows. J. Fluid Mech. 242, 169–192.
Unadkat, H., Rielly, C.D., Nagy, Z.K., 2011. PIV study of the flow field generated by a sawtooth impeller. Chem. Eng. Sci. 66, 5374–5387.
Valente, P.C., Vassilicos, J.C., 2012. Universal dissipation scaling for nonequilibrium turbulence. Phys. Rev. Lett. 108, 214503.
Vassilicos, J.C., 2015. Dissipation in turbulent flows. Annu. Rev. Fluid Mech. 47, 95–114.
Wallace, J.M., Vukoslavčević, P.V., 2010. Measurement of the velocity gradient tensor in turbulent flows. Annu. Rev. Fluid Mech. 42, 157–181.
Wan, D., Yi, X., Wang, L.-P., Sun, X., Chen, S., Wang, G., 2020. Study of collisions between particles and unloaded bubbles with point-particle model embedded in the direct numerical simulation of turbulent flows. Miner. Eng. 146, 106137.
Wang, L.P., Chen, S., Brasseur, J.G., Wyngaard, J.C., 1996. Examination of Hypotheses in Kolmogorov Refined Turbulence Theory through High-Resolution Simulations. Part 1. Velocity Field. Journal of Fluid Mechanics 309, 113–156.
Wang, G., Evans, G.M., Jameson, G.J., 2016a. Experiments on the detachment of particles from bubbles in a turbulent vortex. Powder Technol. 302, 196–206.
Wang, G., Nguyen, A.V., Mitra, S., Joshi, J.B., Jameson, G.J., Evans, G.M., 2016b. A review of the mechanisms and models of bubble-particle detachment in froth flotation. Sep. Purif. Technol. 170, 155–172.
Wang, G., Sathe, M., Mitra, S., Jameson, G.J., Evans, G.M., 2014a. Detachment of a bubble anchored to a vertical cylindrical surface in quiescent liquid and grid generated turbulence. Can. J. Chem. Eng. 92, 2067–2077.
Wang, G., Wan, D., Peng, C., Liu, K., Wang, L.-P., 2019. LBM study of aggregation of monosized spherical particles in homogeneous isotropic turbulence. Chem. Eng. Sci. 201, 201–211.
Wang, G., Zhou, S., Joshi, J.B., Jameson, G.J., Evans, G.M., 2014b. An energy model on particle detachment in the turbulent field. Miner. Eng. 69, 165–169.
Wiles, P.J., Rippeth, T.P., Simpson, J.H., Hendricks, P.J., 2006. A novel technique for measuring the rate of turbulent dissipation in the marine environment. Geophys. Res. Lett. 33.
Williams, J., Crane, R., 1983. Particle collision rate in turbulent flow. Int. J. Multiphase Flow 9, 421–435.
Worth, N., Nickels, T., 2011. Time-resolved volumetric measurement of fine-scale coherent structures in turbulence. Phys. Rev. E 84, 025301.
Wu, H., Patterson, G., Van Doorn, M., 1989. Distribution of turbulence energy dissipation rates in a Rushton turbine stirred mixer. Exp. Fluids 8, 153–160.
Wu, H., Patterson, G.K., 1989. Laser-Doppler measurements of turbulent-flow parameters in a stirred mixer. Chem. Eng. Sci. 44, 2207–2221.
Xu, D., Chen, J., 2013. Accurate estimate of turbulent dissipation rate using PIV data. Exp. Therm. Fluid Sci. 44, 662–672.
Zaripov, D., Li, R., Dushin, N., 2019. Dissipation rate estimation in the turbulent boundary layer using high-speed planar particle image velocimetry. Exp. Fluids 60, 18.
Zaripov, D., Li, R., Saushin, I., 2020. Extreme events of turbulent kinetic energy production and dissipation in turbulent channel flow: particle image velocimetry measurements. J. Turbulence 21, 39–51.
Zeff, B.W., Lanterman, D.D., McAllister, R., Roy, R., Kostelich, E.J., Lathrop, D.P., 2003. Measuring intense rotation and dissipation in turbulent flows. Nature 421, 146–149.
Zhang, H., Yang, G., Sayyar, A., Wang, T., 2019. An improved bubble breakup model in turbulent flow. Chem. Eng. J.
Zhang, J., Tao, B., Katz, J., 1997. Turbulent flow measurement in a square duct with hybrid holographic PIV. Exp. Fluids 23, 373–381.
Zhou, G., Kresta, S.M., 1996a. Distribution of energy between convective and turbulent-flow for 3 frequently used impellers. Chem. Eng. Res. Des. 74, 379–389.
Zhou, G., Kresta, S.M., 1996b. Impact of tank geometry on the maximum turbulence energy dissipation rate for impellers. AlChE J. 42, 2476–2490.
Zhou, G., Kresta, S.M., 1998. Correlation of mean drop size and minimum drop size with the turbulence energy dissipation and the flow in an agitated tank. Chem. Eng. Sci. 53, 2063–2079.
Zhu, Y., Antonia, R.A., 1996a. Spatial resolution of a 4-X-wire vorticity probe. Meas. Sci. Technol. 7, 1492–1497.
Zhu, Y., Antonia, R.A., 1996b. The spatial resolution of hot-wire arrays for the measurement of small-scale turbulence. Meas. Sci. Technol. 7, 1349–1359.